NTNU – Trondheim
Norwegian University of
Science and Technology

Physical model study on impacts of landslide generated wave action on embankment dams

Matteo Bolzoni

Hydropower Development

Submission date:	June 2015
Supervisor:	Leif Lia, IVM
Co-supervisor:	Kiflom Belete, IVM

Norwegian University of Science and Technology
Department of Hydraulic and Environmental Engineering

NTNU
Norwegian University of Science and Technology

Faculty of Engineering Science and Technology
Department of Hydraulic and Environmental Engineering

M.Sc. THESIS IN HYDROPOWER DEVELOPMENT

Candidate: Matteo Bolzoni

Title: Physical model study on impacts of landslide generated wave action on embankment dams.

1 BACKGROUND

Landslide hazard from mountainsides above reservoirs are a potential threat to embankment dams. A research project that was carried out on the hazards related to landslide showed that many reservoirs and dams in Norway are in landslide prone areas and with potential risk of overtopping due to slid generated waves. NVE has been working on risks associated with landslide and also interested to gain more knowledge about the impact of the landslide generated waves on the embankment dams. This is with an understanding that more knowledge on the subject can be a better foundation for the improvement of methods and regulations with regard to overtopping and other impacts on dams as a result of the waves caused by landslides.

A study program was initiated on impacts of landslide generated wave action on dams by the Norwegian Water Resources and Energy Directorate (NVE) in collaboration with NTNU. The aim was to well understand the impact of landslide generated wave in reservoirs on dams. For this purpose work has been carried out to modify and use for experimental study the large scale physical model of the Åknes/Storfjord which was built in the hydraulic laboratory at NTNU, originally it was built to study landslide generated tsunami waves in fjords.

In 2014 a necessary modification has been made on the Geiranger part of the Storfjord model including building of a dam structure and instrumentation. An experimental study was conducted using the modified model in the hydraulic laboratory by students as part of their thesis. During the experimental test different landslide scenarios was used by varying slide parameters. The physical processes and interaction between the land slide generated waves and dam overtopping was studied. A comparison was also made between the results obtained from the experimental test with results from the computational method recommended by Heller et al. (2009). The preliminary result from this study gave basic insight to the subject matter. However it also recommended need for further study to verify results of the experimental test, as well as testing the influencing parameters by conducting more tests and detailed measurements. Thus, this thesis assignment is plan to conduct further physical model test on the physical model in the lab.

2 MAIN QUESTIONS FOR THE THESIS

The thesis will be composed of a number of tasks related to assessing relevant literature and preparing and running an experimental study on the existing physical model. The main objective of the study is to undertake additional investigation on the scale model in hydraulic laboratory in order to study the effect of landslide generated waves on Embankment dams. This is to gain more knowledge about the impact of landslide generated wave on dams. This knowledge will contribute to the processes of developing a method to calculate the size of the overtopping over an embankment dam as a result of landslide generated wave in reservoirs and also to assess what consequences can have on safety of the embankment dams in general.

2.1 The specific tasks are detailed as follows

1. Review current literature, an important aspect of the review will be to find examples of previous study on landslide generated wave impacts on embankment dam and study the governing parameters, their characteristics and interaction. The literature review will be basis for the initial stages to plan the model study.

2. Study the Geiranger model set-up and the installed instrument. Carry out a model test to study the effect of land slide generated wave on embankment dams. In this case the wave will be generated using a select slide size/volume and the corresponding wave height, overtopping volume and overtopping depth above the dam crest in the model will be measured and studied under different dam arrangement. During the test relevant dam parameters such as upstream dam face slope will be varied. The experimental result will be used to study the physical processes and the relationship between
    - The slide volume and generated wave height
    - The wave height and dam overtopping volume
    - Different dam face slope and overtopped volume

3. The results from the model test will be compared with results from the numerical calculation. For this purpose the numerical method from Müller (1995) and reported by Heller.V and Hager.W.H and Minor. H.E, (2009) will be used at the beginning as a base for numerical computation. Further review can also be made to test other numerical methods.

4. Perform a thorough sensitivity and uncertainty analysis of the parameters and identify the limitations and/ possibility for improvement and also draw recommendation for practical application.

3 SUPERVISION, DATA AND INFORMATION INPUT

Professor Leif Lia will be the supervisor of the thesis work. Research scientist Kiflom Belete will provide advice on the process of the study.

Discussion with and input from colleagues and other research or engineering staff at NTNU, SINTEF, power companies or consultants are recommended. Significant inputs from others shall, however, be referenced in a convenient manner.

The research and engineering work carried out by the candidate in connection with this thesis shall remain within an educational context. The candidate and the supervisors are therefore free to introduce assumptions and limitations, which may be considered unrealistic or inappropriate in a contract research or a professional engineering context.

4 REPORT FORMAT AND REFERENCE STATEMENT

The thesis report shall be in the format A4. It shall be typed by a word processor and figures, tables, photos etc. shall be of good report quality. The report shall include a summary, a table of content, lists of figures and tables, a list of literature and other relevant references and a signed statement where the candidate states that the presented work is his own and that significant outside input is identified.

The report shall have a professional structure, assuming professional senior engineers (not in teaching or research) and decision makers as the main target group.

The summary shall not contain more than 450 words it shall be prepared for electronic reporting to SIU. The entire thesis may be published on the Internet as full text publishing through SIU. The candidate shall provide a copy of the thesis (as complete as possible) on a CD in addition to the A4 paper report for printing.

The thesis shall be submitted no later than **10th of June 2015.**

Trondheim 6th of February 2015

____

Leif Lia

Professor

Forewords

This Master's thesis titled "Physical model study on impacts of landslide generated wave action on embankment dams" has been written in collaboration with the Department of Hydraulic and Environmental Engineering at NTNU and the Norwegian Water Resources and Energy Directorate (NVE).
It is carried out under the supervision of Professor Leif Lia, Department of Hydraulic and Environmental Engineering, Norwegian University of Science and Technology, Trondheim, Norway.

The thesis work started in January 2015 and was completed in June 2015.

I hereby confirm that all the work carried in this thesis is my own and significant outside efforts have been acknowledged.

Matteo Bolzoni
June 2015
Trondheim, Norway

Acknowledgment

I would like to express my deep gratitude to my supervisor Leif Lia for giving me the possibility of working on this interesting and challenging project and for his useful comments and remarks. Furthermore, I would like to thank Professor Kiflom Belete for his precious help and support. I am also extremely grateful to Geir Tesaker for his valuable assistance in the laboratory.

Matteo Bolzoni

Trondheim, 10.06.2015

Summary

The master thesis "Physical model study on impacts of landslide generated wave action on embankment dams" has been written in collaboration with the Department of Hydraulic and Environmental Engineering at NTNU and the Norwegian Water Resources and Energy Directorate (NVE). The thesis focuses on studying the effects of landslide generated waves on embankment dams in order to estimate safe freeboards. A landslide falling into a reservoir produces impulsive waves than can have catastrophic consequences to the reservoir sidewalls, the dam body and, in case of overtopping, endanger human activities downstream of the dam. Therefore, the investigation of landslide hazard and risk on reservoir banks is of the utmost importance.

The tests were conducted at the scaled model of the Viddal reservoir (Norway) and slide velocity, wave height from 10 stations, overtopping height on the dam crest and overtopping volume have been collected. In total 17 tests were conducted varying the following parameters: slide volume (2, 4 and 6 blocks), freeboard (30 mm and 80 mm) and dam slope (1:1.6, 1:2 and 1:2.4); in addition for the two last tests the dam roughness was varied by gluing stones on the upstream dam slope. The impacts of these parameters on the run-up height and the overtopping volume have been studied; moreover, the processes of wave propagation and run-up have been discussed. The run-up height and the overtopping volume monitored during the tests have then been compared with the results calculated with the Heller's numerical method. The calculation method uses 15 governing parameters to compute the overtopping volume and the run-up height caused by subaerial landslide generated waves. The parameters can easily be measured in the model. Moreover, the method enables to calculate the desired results for both 2D and 3D reservoir geometry.

The collected results show a strong correlation between the overtopping volume and the slide volume. It was also noticed the great influence of the freeboard on the overtopping size. Even though only two tests were performed, the impact of the upstream dam slope roughness was found to be significant. On the other hand, the influence of the dam slope is minor, causing only slight changes in the overtopping volume.

The results obtained using the Heller's method show large discrepancies between observed and simulated data. The main reason is the method assumption of an idealized reservoir geometry which strongly differ from the model shape. It is thus concluded that the Heller's method cannot be applied to the Viddal reservoir and reservoirs with similar geometry, in order to determine a safe freeboard.

Index of contents

List of figures

List of tables

1 Introduction

1.1 Motivation

In recent years, the investigation of landslide hazard and risk has been a major research focus for the international community, in particular with the booming of dam constructions all over the world, large landslides on reservoir banks have nowadays become a highly sensitive issue.
A landslide falling into a reservoir produces impulsive waves than can have catastrophic consequences to the reservoir sidewalls, the dam body and, in case of overtopping, endanger human activities downstream of the dam.
Landslides in reservoir are mainly caused by the bad hydrodynamic conditions of slope banks during the period of reservoir water level changing and rainfall infiltration. Instability of the bank slopes has been a challenging issue for the construction of hydropower projects, in the last decades the need for understanding this complex phenomenon has become of the utmost importance after several destructive incidents.
One of the most known landslide disaster happened at the Vajont reservoir, in Italy. The 9 October 1963 a 300 million m^3 landslide originated from the nearby mountain fell into the reservoir creating an 80-m-high wave that overtopped the arch dam and destroyed the villages downstream killing over 2000 people.

Figure 1-1 Vajont dam site after the disaster

However, in the reservoir area an even higher wave height was registered.

A well-known landslide case in Norway happened in Tafjord in 1934 where a 1.5 million m^3 sub-aerial rockslide originated a 15-m-high tsunami like wave killing 40 people.

Figure 1-2 Tafjord area after the landslide

Norway generates 95% of its electricity from hydropower plants; therefore, the assessment of the reservoir banks stability is fundamental. The risk of potential landslides in Norwegian reservoirs is the focus of the NVE in order to have a better understanding on the subject as well as for improving safety regulations regarding the potential dam overtopping.

1.2 Objectives

The aim of the master thesis "Physical model study on impacts of landslide generated wave action on embankment dams" by the Norwegian Water Resources and Energy Directorate (NVE) is to gain more knowledge about the impact of landslide generated waves on dams particularly regarding the size of the overtopping. During the tests important parameters such as slide volume, upstream dam slope and roughness were varied and the effects that these have on the dam have been studied. In addition, the results from the model tests were compared with the results from the Heller's numerical method as a base for numerical computation.

1.3 Methodology

Literature review has been the basis in order to plan the model study. Subsequently a thorough physical model testing has been done; the collected results from the tests have then been compared with the simulated data from the Heller's numerical method. Final conclusions and recommendations are then presented.

2 Theoretical background on landslide and impulse waves

Impulse waves are classified as gravity waves and they can be generated after landslides, rockfalls, shore instability, avalanches, glacier calvings. They can both occur in open sea as well as in closed areas such as a reservoir or a lake.

Mass movements can be triggered by a great variety of events such as earthquakes, intense rainfall and rapid changes in the water level of reservoirs (Schuster and Wieczorek, 2002).

Mass movements can be of different kind depending on the material (solid body or granular), and the movement type.

Varnes (1958) identified five mass movement types: sliding, flowing, falling, toppling and spreading.

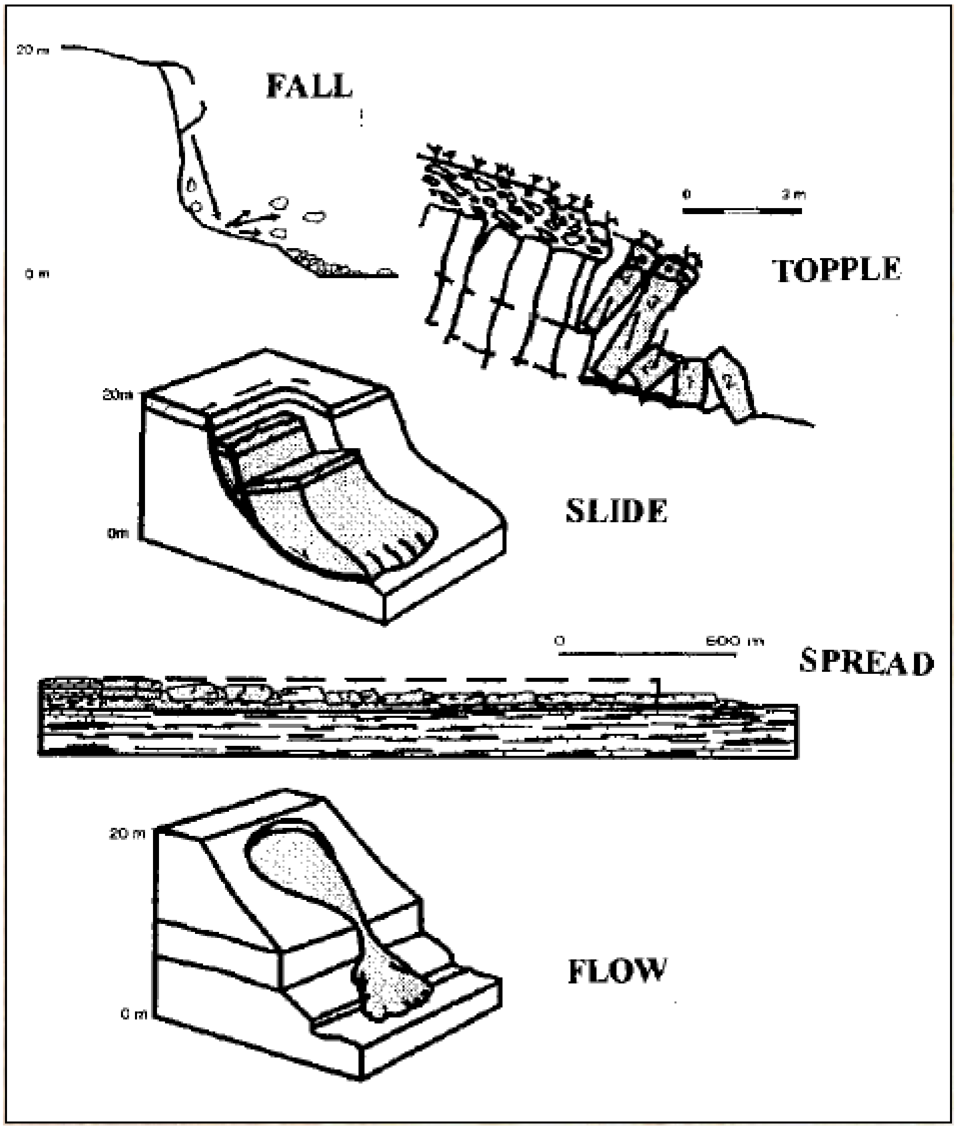

Figure 2-1 Mass movement types (Varnes, 1958)

Slides can also be classified depending on the starting position of the slide body, three different slide categories are then identified: subaerial, partially submerged and submerged.

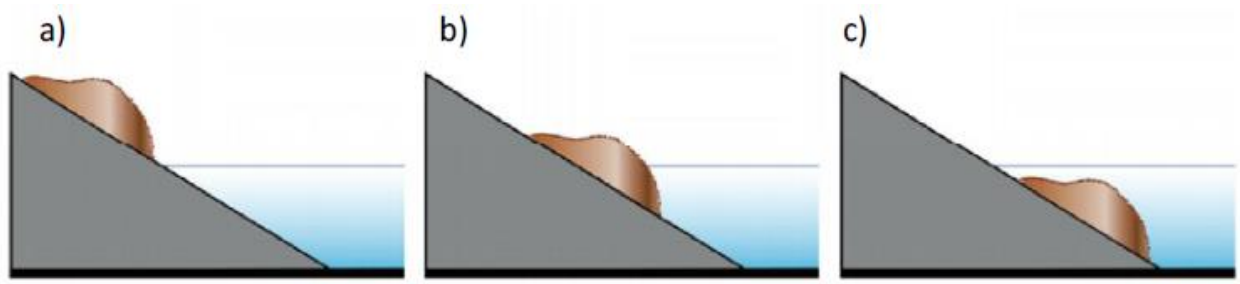

Figure 2-2 Starting positions of landslides: a) subaerial; b) partially submerged; c) submerged (Heller et al., 2009)

In this thesis only solid subaerial slide has been considered.

An impulse wave generated in a reservoir has three distinct phases:

- Wave generation due to slide impact
- Wave propagation
- Wave run-up and dam overtopping

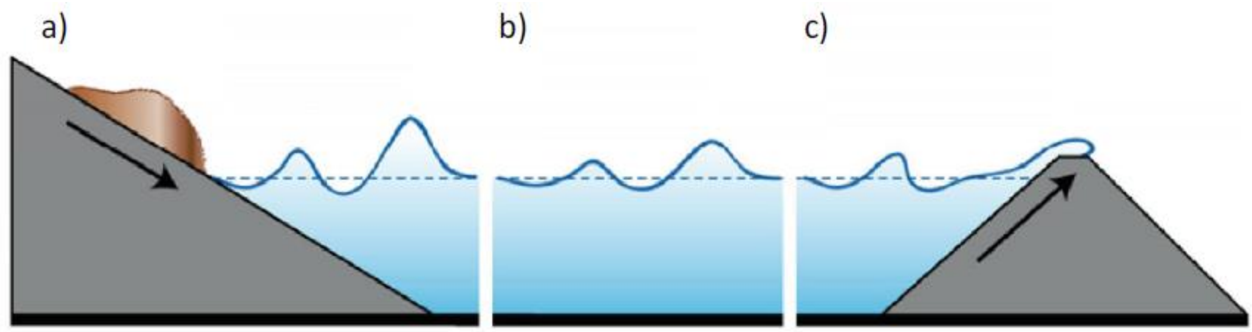

Figure 2-3 Phases of landslide generated waves: a) wave generation due to slide impact; b) wave propagation; c) wave run-up and overtopping (Heller et al., 2009)

Landslide generated impulse waves are non-periodic, non-linear waves; therefore, they greatly differ from the ideal sinusoidal wave. Heller (2009) identifies impulse waves into one of these four groups: Stokes wave, cnoidal wave, solitary wave and bore.

The parameter used to describe a wave are the following:

a - wave amplitude [m]

c - wave celerity [m/s]

h - still water depth [m]

H - wave height [m]

L - wave length [m]

T - wave period [s]

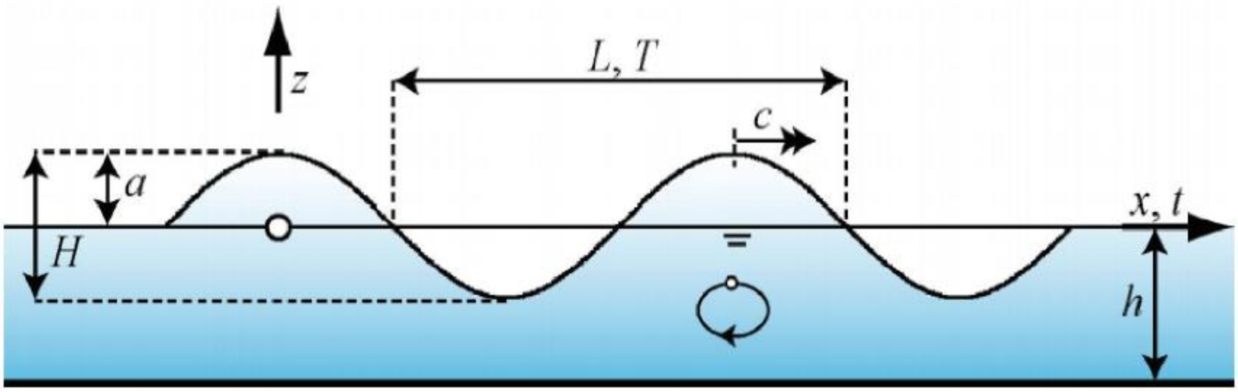

Figure 2-4 Ideal sinusoidal wave

- Stokes wave

It is a deep/intermediate water wave with a steeper profile than the ideal sinusoidal wave and a low fluid mass transport.

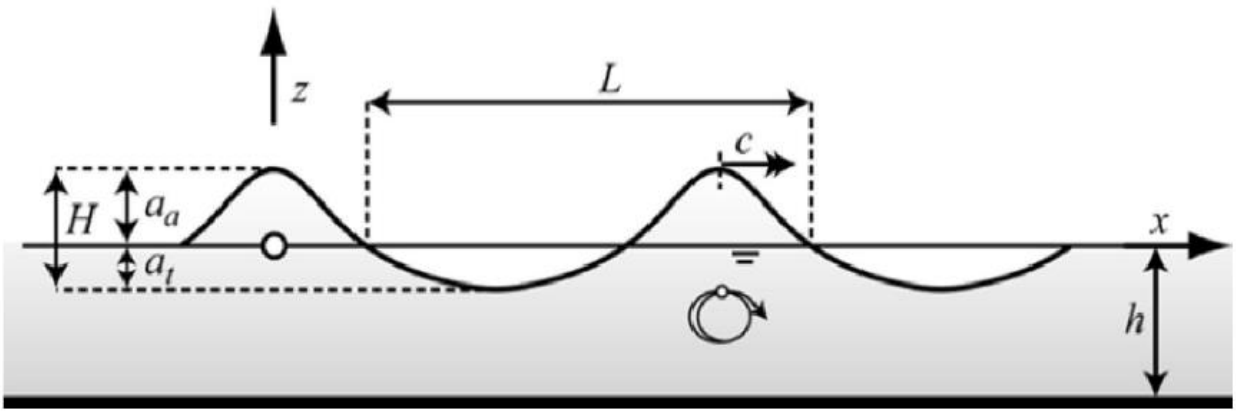

Figure 2-5 Stokes wave

- Cnoidal wave

It is a periodic wave found in intermediate/shallow water, the cnoidal wave has an oscillator character and a low fluid mass transport.

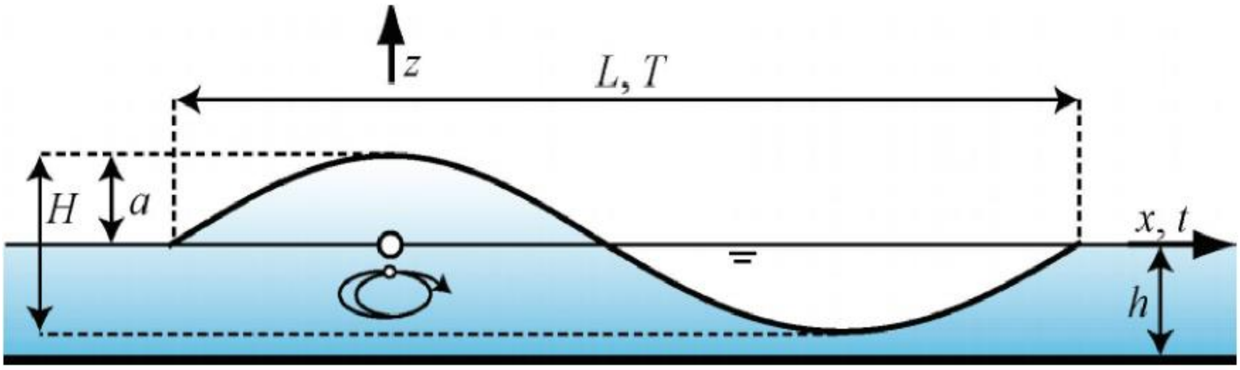

Figure 2-6 Cnoidal wave

- Solitary wave

It is a shallow water wave consisting only of a wave peak with no trough; therefore, the wave amplitude is equal to the wave height. The solitary wave, also called tsunami wave, has a constant wave height and thus the fluid mass transport is huge.

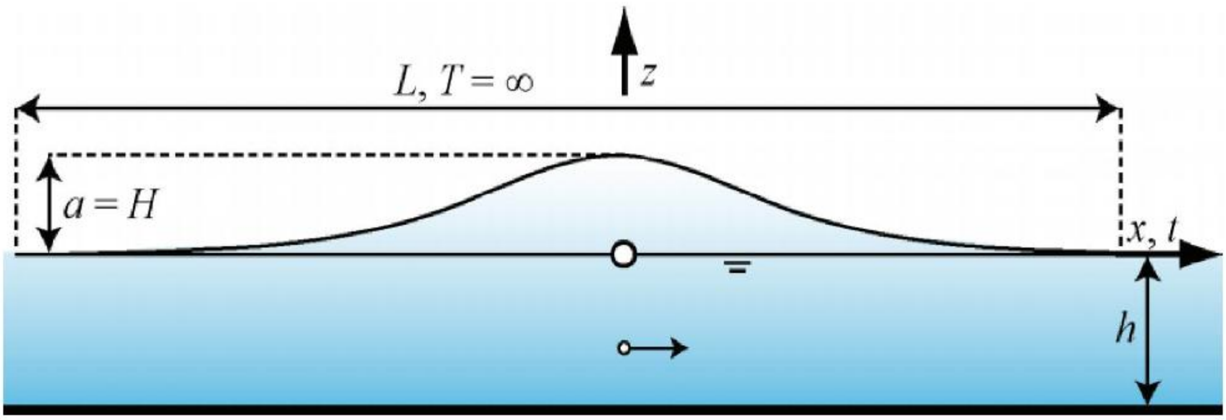

Figure 2-7 Solitary wave

- Bore

It is a shallow water wave created during the wave breaking near the shore. The bore has a steep front and a horizontal movement enabling it to have a massive fluid mass transport.

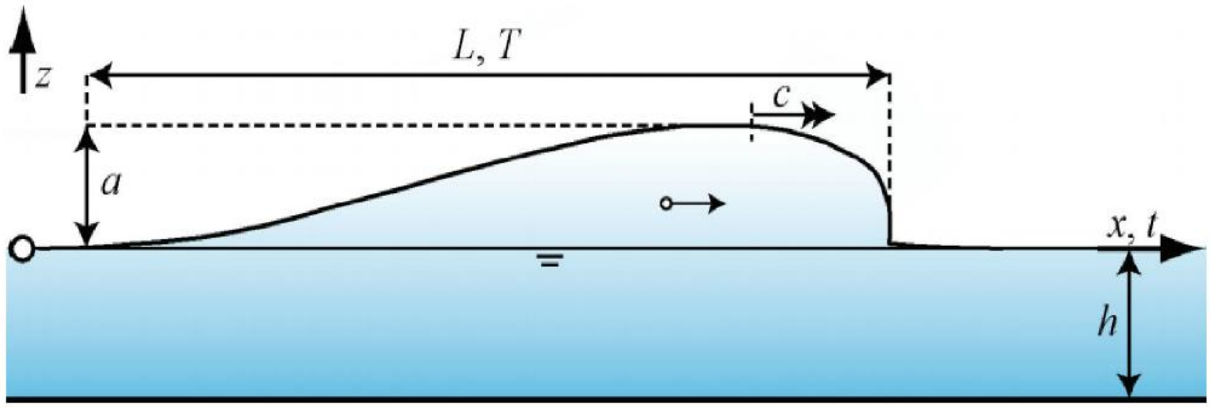

Figure 2-8 Bore

2.1 Literature review on landslide generated waves and their impacts on dams

As mentioned before the first phase of an impulse wave is the wave generation due to the slide impact with the water, the governing parameters that have an influence on the generated wave characteristics are:

V_s - slide impact velocity [m/s]

V - slide volume [m^3]

s - slide thickness [m]

b - slide width [m]

ρ_s - slide density [g/cm^3]

n - slide porosity [%]

α - slide impact angle [°]

h - still water depth [m]

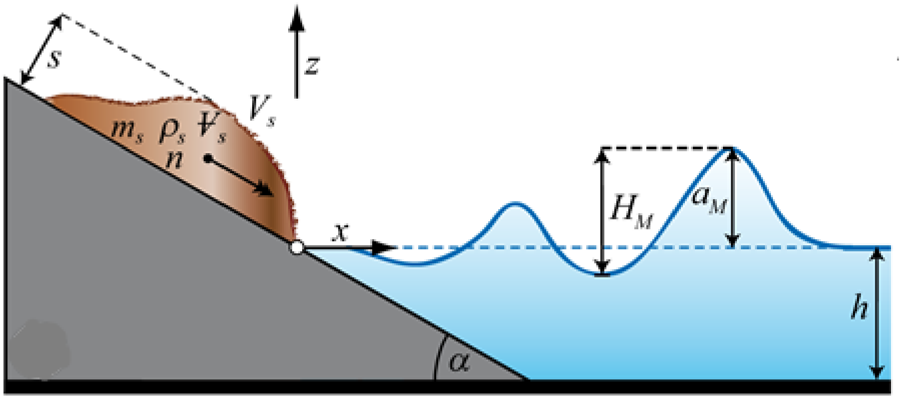

Figure 2-9 Governing parameters on impulse wave generation (Heller et al., 2009)

The influence of the slide front angle on the impulse wave generation was tested by Kamphuis and Bowering (1972) whom conducted several tests with a solid body slide in a 45-m-long channel varying most of the governing parameter; it was later found that the slide front angle had a negligible effect. These authors also proposed to apply the solitary wave celerity formula for calculating the speed of the impulse wave, which is found by:

$$c = \sqrt{[g(h + a)]}$$

with:

a - wave amplitude [m]

c - wave celerity [m/s]

h - still water depth [m]

g - gravitational acceleration [m/s^2]

During tests with a solid body slide in a wave basin Panizzo et al. (2005) introduced the time of underwater slide motion as an additional governing parameter, however, since it was difficult to estimate it had to be calculated empirically as a function of the remaining parameters. The authors also proposed formulas to calculate the maximum wave height and the corresponding maximum wave period for the 3D case.

The last phase of an impulse wave is the wave run-up due to the impact of the wave with the dam or the shore and the eventual overtopping in case of a dam.

The governing parameters that affect the run-up height and the overtopping volume are:

H - wave height [m]

a - wave amplitude [m]

L - wave length [m]

T - wave period [s]

h - still water depth [m]

β - dam face slope [°]

f - freeboard [m]

b_k - crest width [m]

- dam surface roughness
- dam surface permeability
- wave breaking type
- reservoir geometry
- incidence wave angle

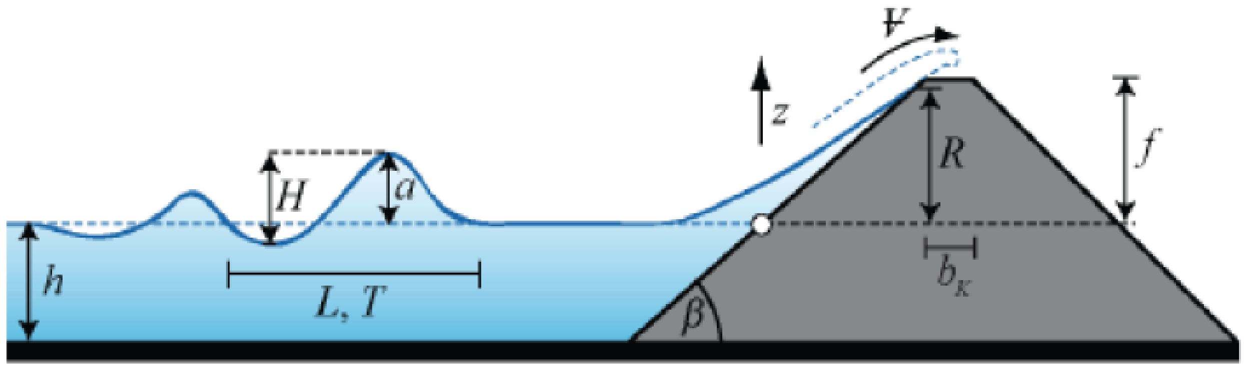

Figure 2-10 Governing parameters on wave run-up and dam overtopping (Heller et al., 2009)

Müller and Vischer (1996) determined a formula for calculating the run-up height in a 2D case; the method was tested by conducting several tests in both wave channel and wave basin with three different dam slopes. As the formula had a deviation of ±10% the applicability of the formula was confirmed, however, it was not possible to integrate it for the 3D case.

The effect of the bed friction on the run-up height was investigated by Teng et al. (2000) whom conducted several tests with both smooth and rough surfaces for three different run-up angles

(10°, 15°, 20°). The authors found out that while for a run-up angle of 20° the roughness had a negligible effect, for 15° and 10° the run-up height was 30% and 50% respectively lower than for a smooth bed.

2.2 Model theory

A physical model is a miniature reproduction of a physical system used for design of hydraulic structures and hydraulic research. A fundamental requisite for physical modelling is the correct design of the model, the scale ratios between model and prototype must be met in order for the model to give a similar response as the prototype. It is therefore important to have geometric, kinematic and dynamic similarity between model and prototype. However, since it is physically impossible to satisfy all force ratios, only the most important ones are related while the others are neglected; this approximation creates differences between model and prototype response (scale effects). Depending on which forces are the most dominant in the process, different scaling criterion are applied:

- Froude similarity: used for gravity driven flows where inertial and gravity forces dominate, typically applied for models of rivers and hydraulic structures.
- Reynolds similarity: used for flows with high internal friction where inertial and viscous forces are significant.
- Euler similarity: used for flows through turbines and pumps where the pressure forces are the most important
- Weber similarity: used for aerated flows where surface tension forces are significant

3 Experiments

The objective of the tests is to study the impacts of landslide generated waves on embankment dams. During the tests slide and dam parameters have been varied in order to study the different impacts on the dam.

The tests were conducted at the Department of Hydraulic and Environmental Engineering at NTNU using the already existing Geiranger model. The model is scaled 1:158 using the Viddal reservoir as a prototype and has a dam located at one end to reproduce artificial reservoir characteristics.

Figure 3-1 Viddal reservoir with location of potential landslide (Lorås, 2014)

3.1 Experimental setup

As mentioned before the model is scaled 1:158 and has a total length of 21 m even though the measurements were taken in the 6 m straight section where the dam is located. The model has different water depths and widths throughout its section which will be shown in the sketch below.

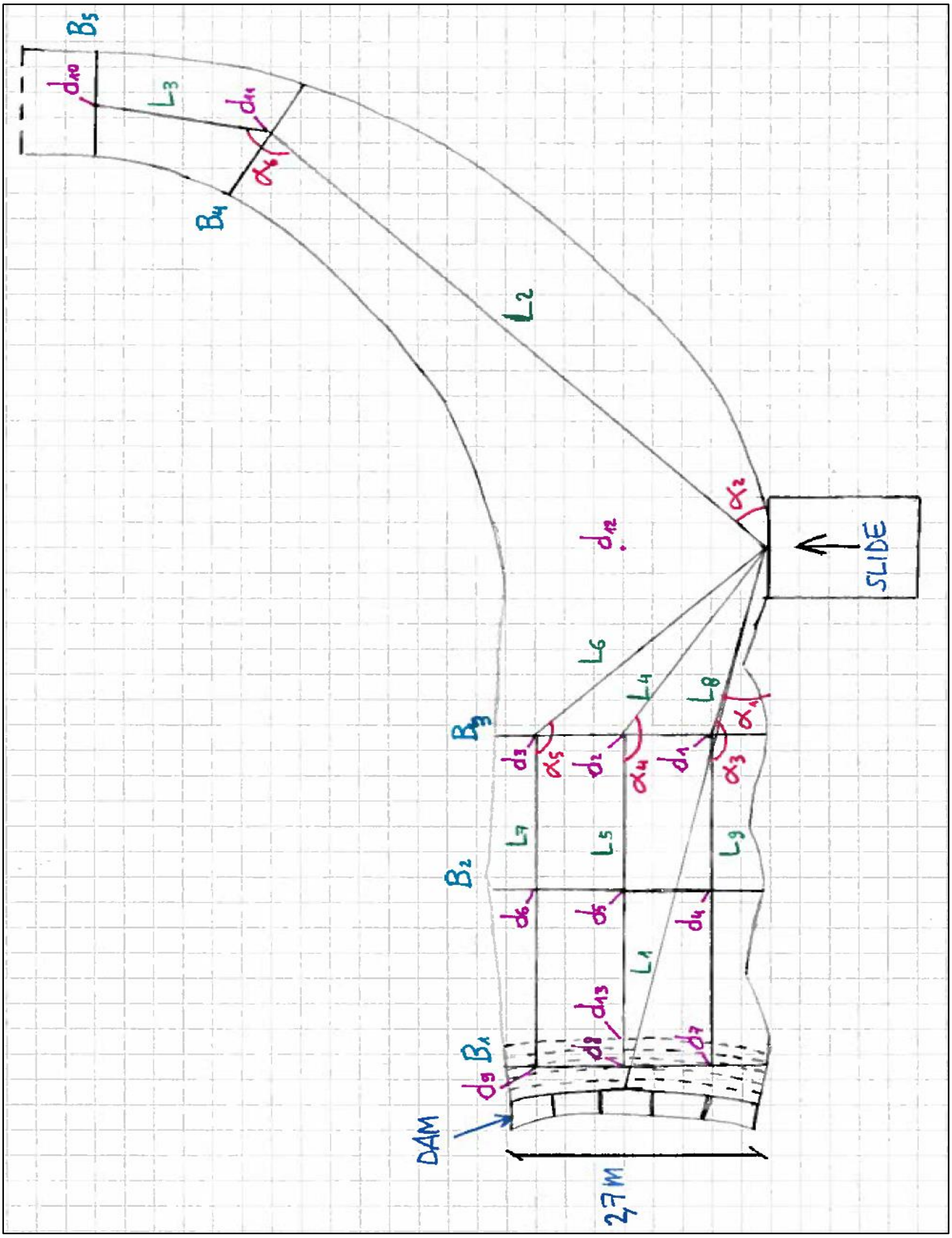

Figure 3-2 Model sketch: planar view

The sketch in Figure 3-2 shows the Geiranger model used in the 17 tests carried out in this work.

In Table 3-1 the geometry of Figure 3-2 will be given.

Table 3-1 Model measurements and prototype proportions

	Width [m]			Length [m]			Depth [m]			
No.	**Model**	**Prototype**	**No.**	**Model**	**Prototype**	**No.**	**Model**	**Prototype**	**No.**	**Angle [°]**
B1	2.605	411.6	L1	6.4	1011.2	d1	0.43	67.94	α1	9
B2	2.92	461.4	L2	9.4	1485.2	d2	0.48	75.84	α2	50
B3	2.74	432.9	L3	2.52	398.2	d3	0.45	71.1	α3	143
B4	1.75	276.5	L4	2.64	417.1	d4	0.3	47.4	α4	142
B5	1.53	241.7	L5	3.52	556.2	d5	0.36	56.88	α5	125
			L6	3.03	478.7	d6	0.35	55.3	α6	140
			L7	3.61	570.38	d7	0.26	41.08		
			L8	2.37	374.5	d8	0.28	44.24		
			L9	3.42	540.4	d9	0.31	48.98		
						d10	0.325	51.4		
						d11	0.325	51.4		
						d12	0.53	83.7		
						d13	0.36	56.9		

17 tests were conducted using different slide volume, freeboard, upstream dam slope and roughness. During each test the slide velocity, wave height, overtopping height and overtopping volume were measured.

3.2 Model setup

The landslide mechanism (Figure 3-4) is composed by a slide ramp where it is possible to place rectangular blocks of different size and weight. The blocks are attached to each other with chains, the slide body is then attached to a steel panel with a hook. In order to measure the speed of the slide a speedometer is connected to the chains (Figure 3-9).

When the hook is removed the blocks slide down on the 42° ramp, after impacting the water a slip mat gradually stops the slide body from further sliding protecting the model bottom at the same time. To start a new test the blocks are then connected to a winch which lifts the slide body in its original position.

The waves generated by the slide trespass the wave sensors (Figure 3-10) hitting on the model banks until some overtop the dam (Figure 3-5). The overtopping volume is collected in five buckets located behind the dam enabling the identification of the most loaded dam sections (Figure 3-8).

In Figure 3-3 the main components of the model are shown.

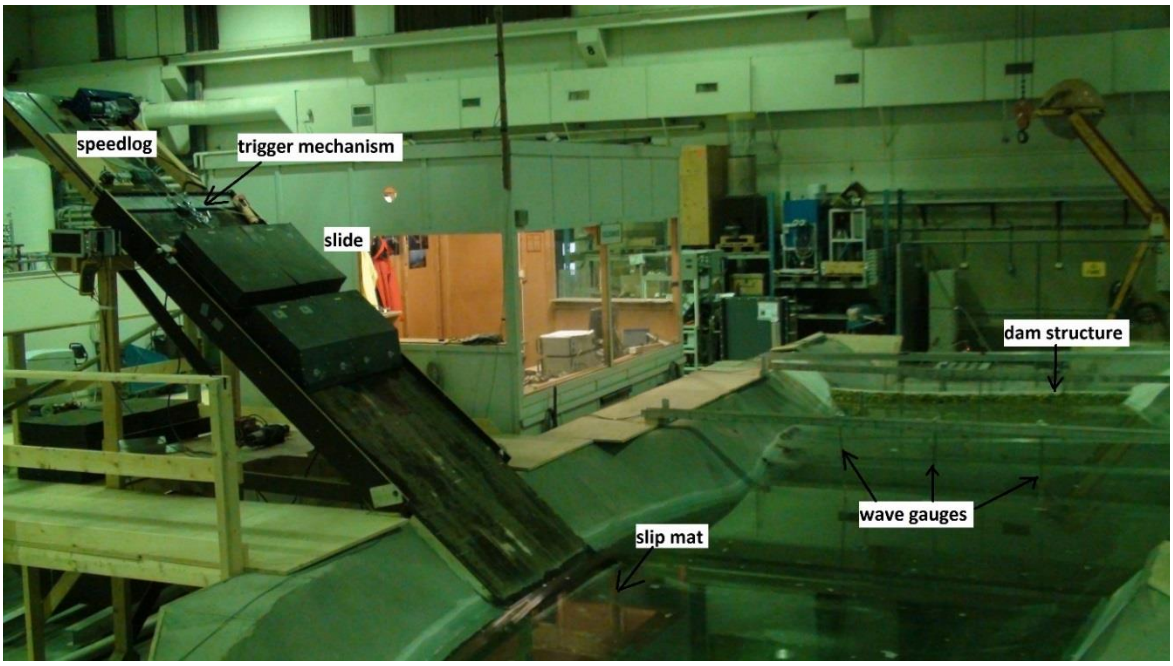

Figure 3-3 Model setup

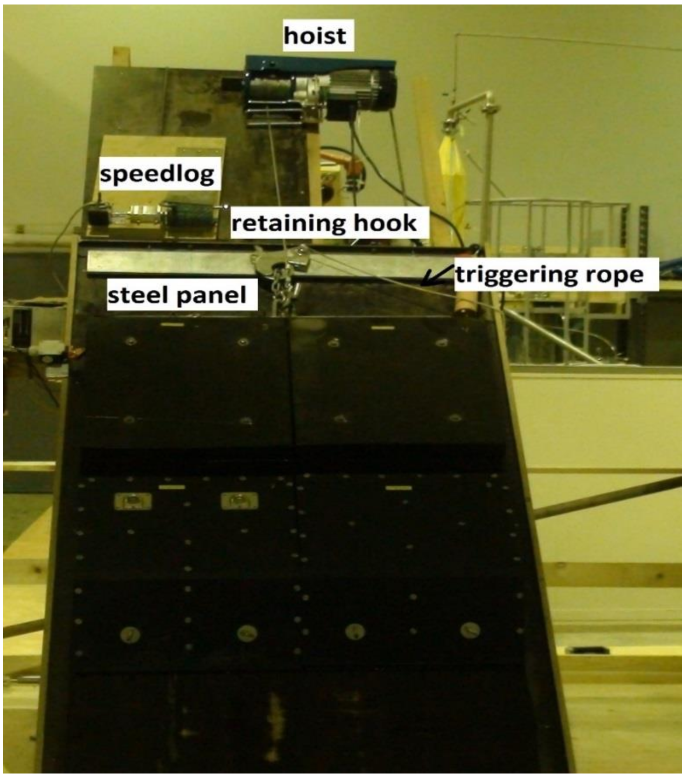

Figure 3-4 Slide mechanism

The main elements of the slide mechanism are shown in Figure 3-4.

The dam structure is presented in Figure 3-5.

Figure 3-5 Dam structure

Figure 3-6 Dam structure with increased roughness

Figure 3-6 shows the dam structure with glued stones on the upstream dam slope.

A detailed sketch of the dam is shown in Figure 3-7.

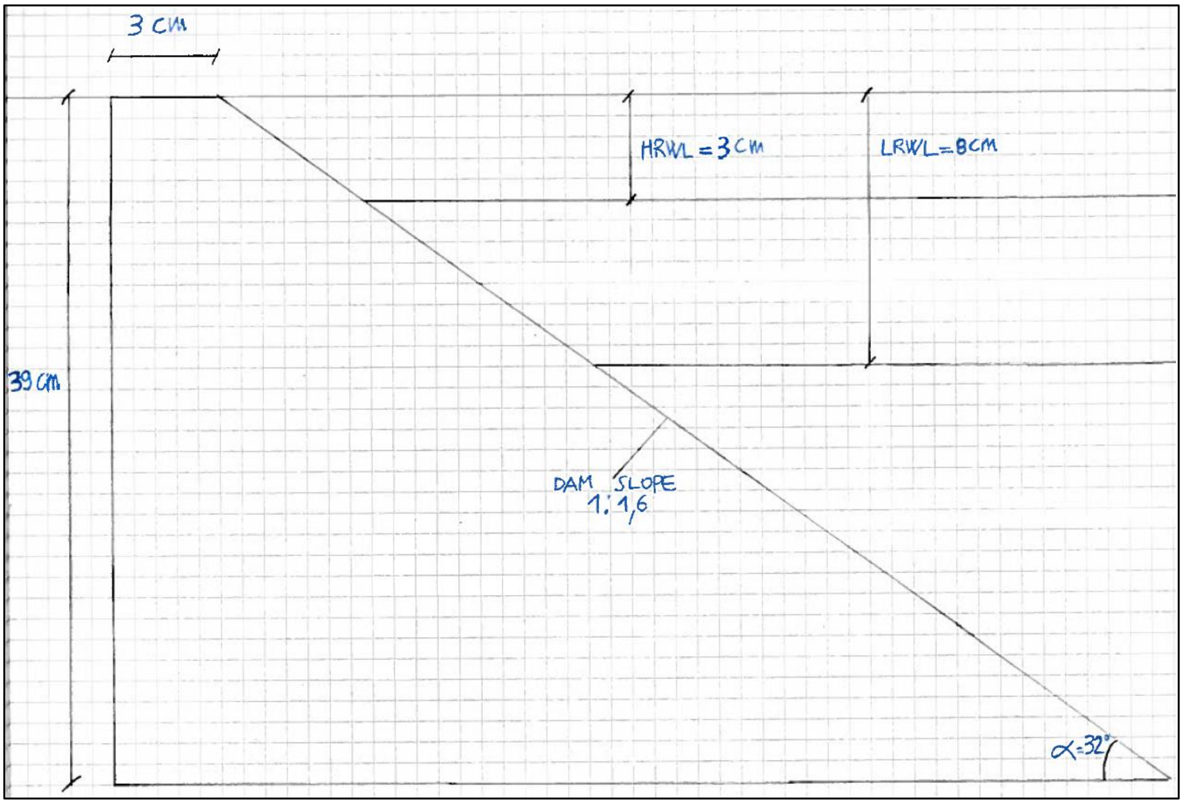

Figure 3-7 Dam sketch

Figure 3-8 Collection buckets and outlets

Figure 3-8 shows the arrangement for collecting the overtopping volume.

3.3 Measurement devices

Several measurement devices were used to collect data:

- Rotational sensor to measure the slide velocity
- Wave gauges to measure the wave height
- Ultrasonic sensors to measure the overtopping
- Camera to record the slide

3.3.1 Rotational sensor

A rotational sensor determines the slide velocity, when the slide body is in the starting position the carbine and the rope of the sensor are attached to the slide's chain. For calibration purposes the voltage of the sensor was first measured in its original position and then measured again when the rope is pulled off 1 m. Potential and distance were then used to calculate the speed in m/s.

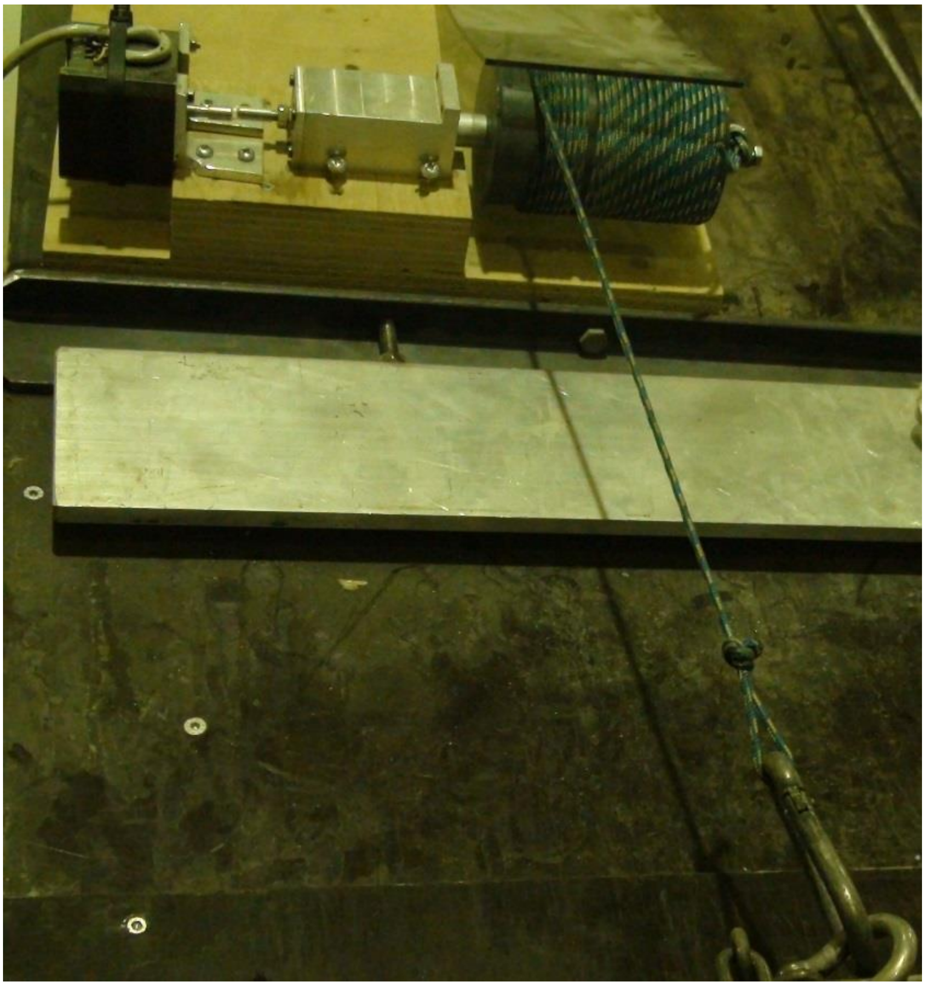

Figure 3-9 Rotational sensor

3.3.2 Wave gauges

The model has 10 wave sensors (DHI Wave-Meter 102E) used to record the wave height, they are mainly located between the slide and the dam, while one is placed after the first bend. The exact location of the gauges is shown in the model sketch.

The working principle of the sensors is based on the electrical conductivity of two parallel electrodes in a fluid. Each wave gauge is connected to a storage device (Agilent U2300A USB) via its own channel transferring the data with a sampling rate of 200 Hz per channel. The software "Agilent Measurement Manager" (AMM) then enables to read the transferred data of the gauges (.csv files) on the computer.

The calibration of the sensors was done in the following way using a voltmeter:

first the steel bars were placed on a 50 mm thick wooden blocks setting the wave sensors to 0 V, afterwards the steel profiles were heightened by 50 mm setting the voltage to -2.5 V to resemble the most negative wave height and then lowered by 50 mm increasing the voltage to +2.5 V to resemble the highest surface elevation.

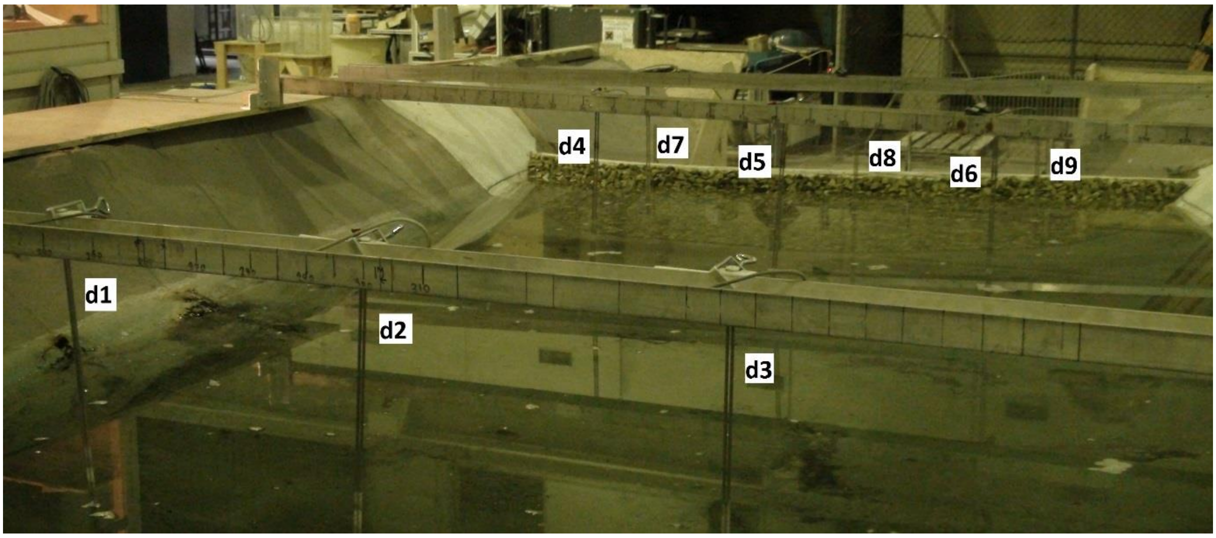

Figure 3-10 Wave gauges

The data collected by the wave gauges are then transferred to a storage device.

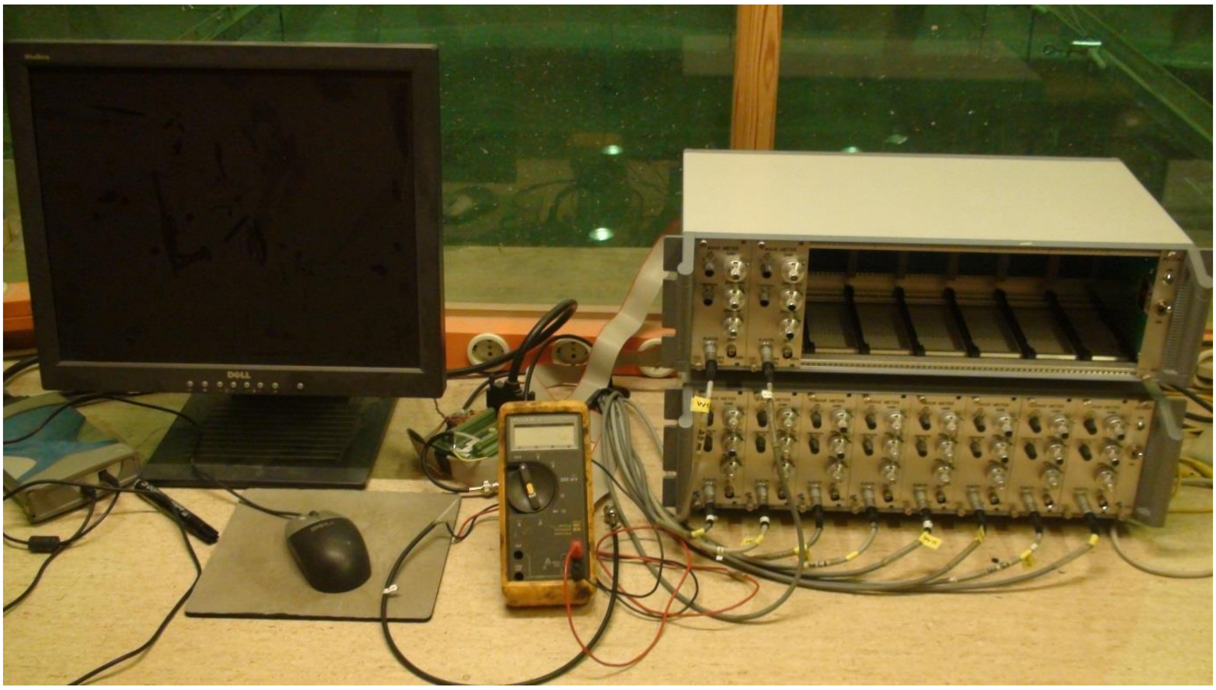

Figure 3-11 Wave channels

3.3.3 Ultrasonic sensors

Two ultrasonic sensors (mic+35/IU/TC) were used to determine both the overtopping height on the dam crest and the overtopping volume in the buckets.

The working principle of the sensors is based on echo-delay giving the distance between the sensor and the reflecting object as a result. To determine the overtopping height the difference between the distance without water and the one during the test is then calculated. A volume-distance curve was plotted to obtain the overtopping volume.

Figure 3-12 Overtopping sensor

3.3.4 Camera

Two cameras were used to record the slide, one was placed next to the dam crest to record the overtopping while the second one was positioned opposite to the dam to record the slide impact.

4 Procedure and tests

4.1 Procedure

Before each test the slide body was prepared on the ramp, the measurement devices connected and calibrated and the camera turned on; then the process could start by simply pulling the rope attached to the hook of the slide blocks. To avoid inaccurate data of the wave gauges the water surface had to be motionless.

4.2 Tests

17 tests were conducted varying the following parameters:

- slide volume: 2, 4 and 6 blocks
- freeboard: 30 mm (identified as HRWL) and 80 mm (identified as LRWL)
- dam slope: 1:1.6, 1:2 and 1:2.4

The first dam slope corresponds to the Viddal dam, while 1:2 and 1:2.4 have been chosen as they represent typical dam slopes in Norway.
In addition for the two last tests it was decided to vary the dam roughness by gluing stones on the upstream dam slope.

Since the gravity effect is the most dominant during the process, the Froude scaling was used for the prototype scaling (1:158).
The tables summarizing the slide characteristics for each test can be found in the Appendix A.

5 Data analysis and discussion of the results

In this chapter, the main results and observations collected during the tests are analyzed and discussed.

5.1 Run-up height

As the freeboard and the dam slope are fundamental parameters that affect the run-up process, detailed sketches of the dam are presented below for the different configurations.

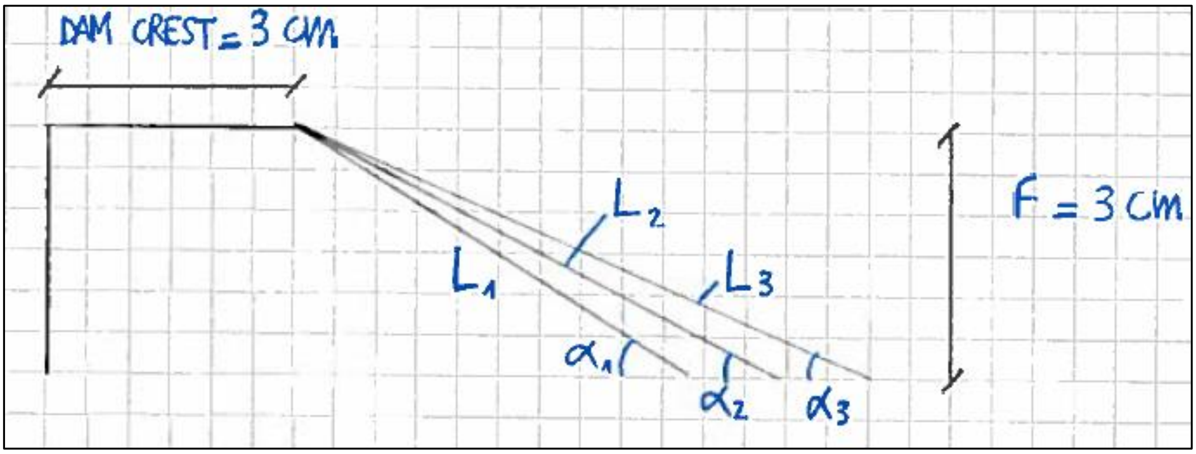

Figure 5-1 Dam configurations in HRWL case

Table 5-1 Dam measurements in HRWL case

HRWL				
Dam slope	**Run-up angle**	**No.**	**Model [m]**	**Prototype [m]**
1 : 1.6	32°	L1	0.06	8.94
1 : 2	26.57°	L2	0.07	10.60
1 : 2.4	22.62°	L3	0.08	12.32

Table 5-1 describes the dam geometry in the HRWL case.

The dam configurations in the LRWL case are shown in Figure 5-2.

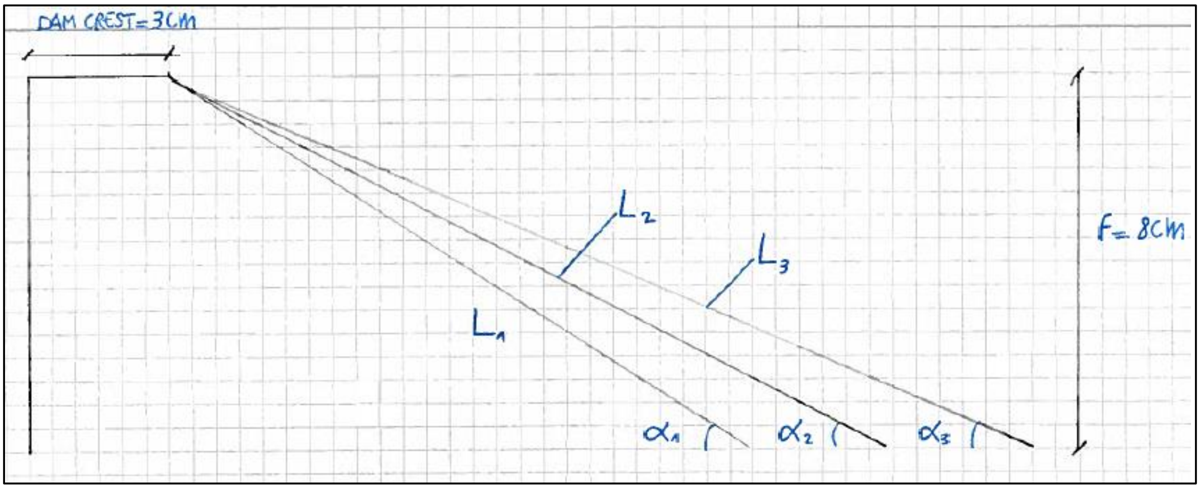

Figure 5-2 Dam configurations in LRWL case

Table 5-2 Dam measurements in LRWL case

LRWL				
Dam slope	**Run-up angle**	**No.**	**Model [m]**	**Prototype [m]**
1 : 1.6	32°	L1	0.15	23.85
1 : 2	26.57°	L2	0.18	28.26
1 : 2.4	22.62°	L3	0.21	32.86

The Table 5-2 describes the dam geometry in the LRWL case.

Figure 5-3 shows the run-up height in prototype scale for each test.

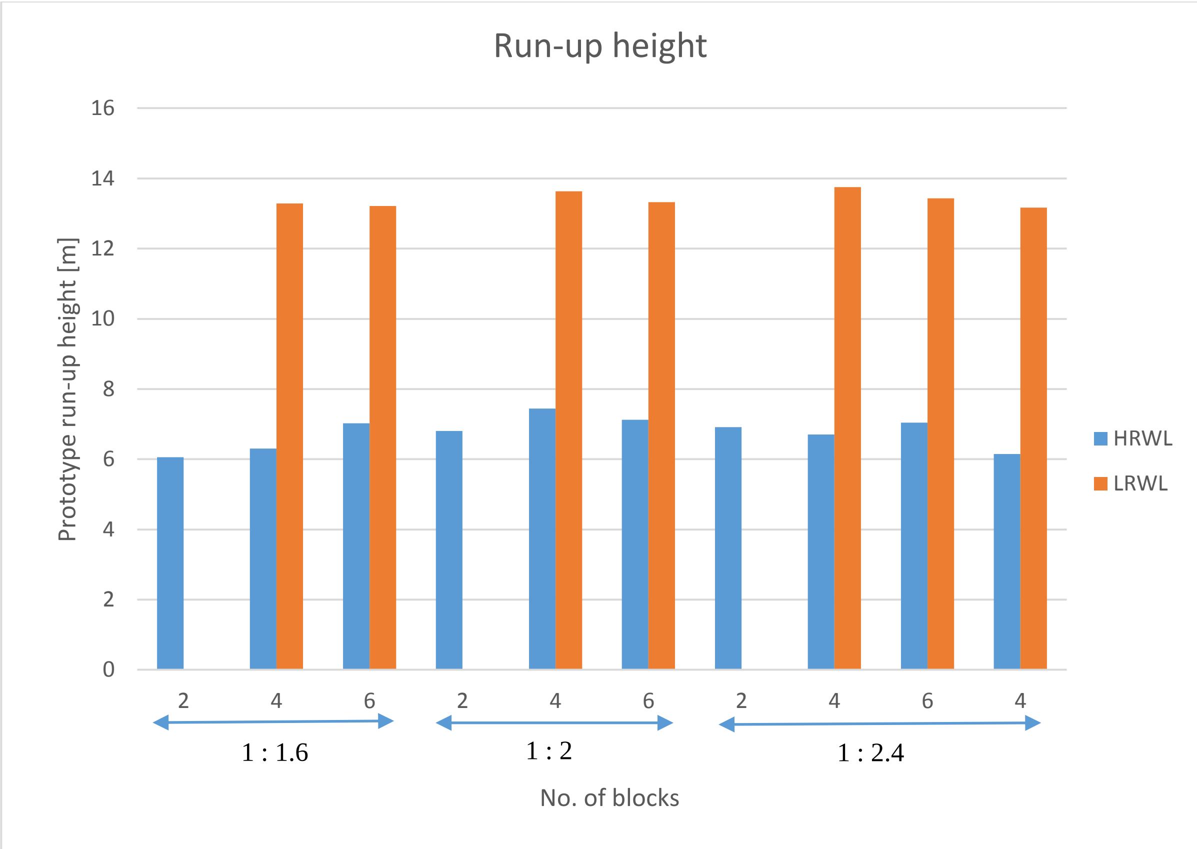

Figure 5-3 Measured run-up height in prototype scale

Analyzing Figure 5-3, it is possible to notice that with the first dam slope the run-up height increases when more blocks are added, while in the other two cases there is no strong correlation between slide volume and run-up height.

The large run-up height difference between the two water levels cases is due to a large increase of the freeboard which is a relevant parameter for the determination of the run-up height.

While in the second dam slope case the run-up height increases compared to the first one, a further decrease of dam slope causes slightly less overtopping. The reason might be due to a not properly smooth upstream dam face when the third dam slope was built that cause loss of energy during the overtopping process.

In the last two cases the change in dam roughness strongly affects the wave run-up causing a significant decrease in run-up height.

The importance of the freeboard on the wave run-up will be discussed below.

5.1.1 LRWL case

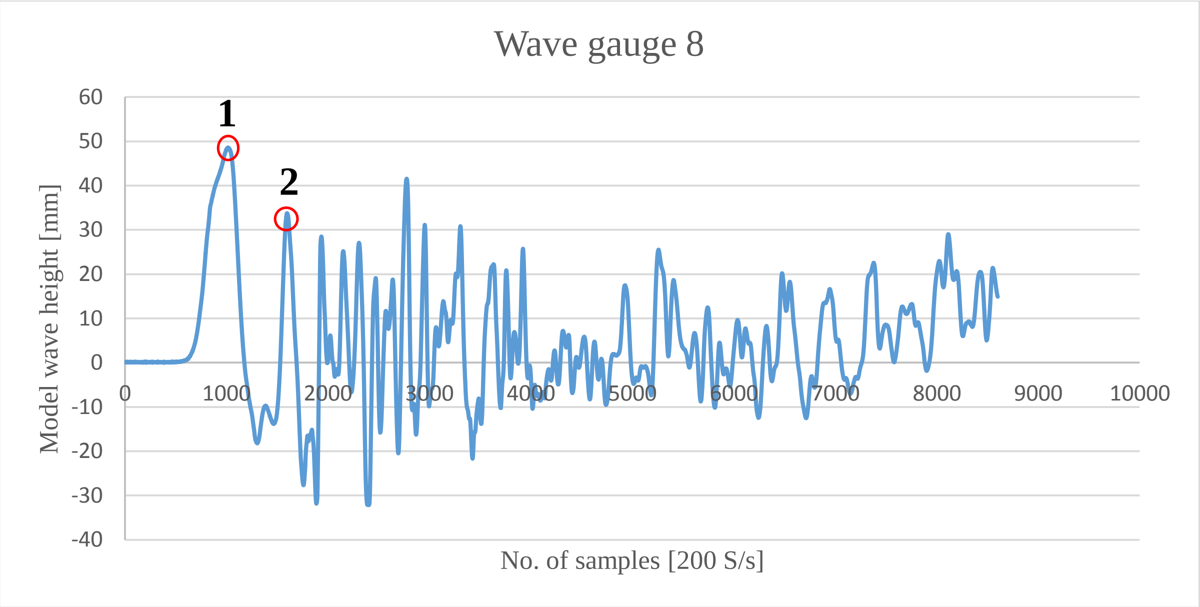

Figure 5-4 Wave gauge 8 measurements in LRWL case

The x-axis is presented by 200 samples per second, which means that 1000 samples equal to 5 seconds.

In the LRWL case, the freeboard is 7.9 m (in prototype) higher compared to the HRWL situation where the traveling distance of the waves on the dam face is considerably shorter.
Analyzing the video and data from the wave gauge 8 (located in central position in front of the dam) it was determined that the wave creating the highest registered overtopping is the first one. The run-up of the second wave is substantially higher than the previous one, causing loss of energy during the process and consequently a smaller wave height.

5.1.2 HRWL case

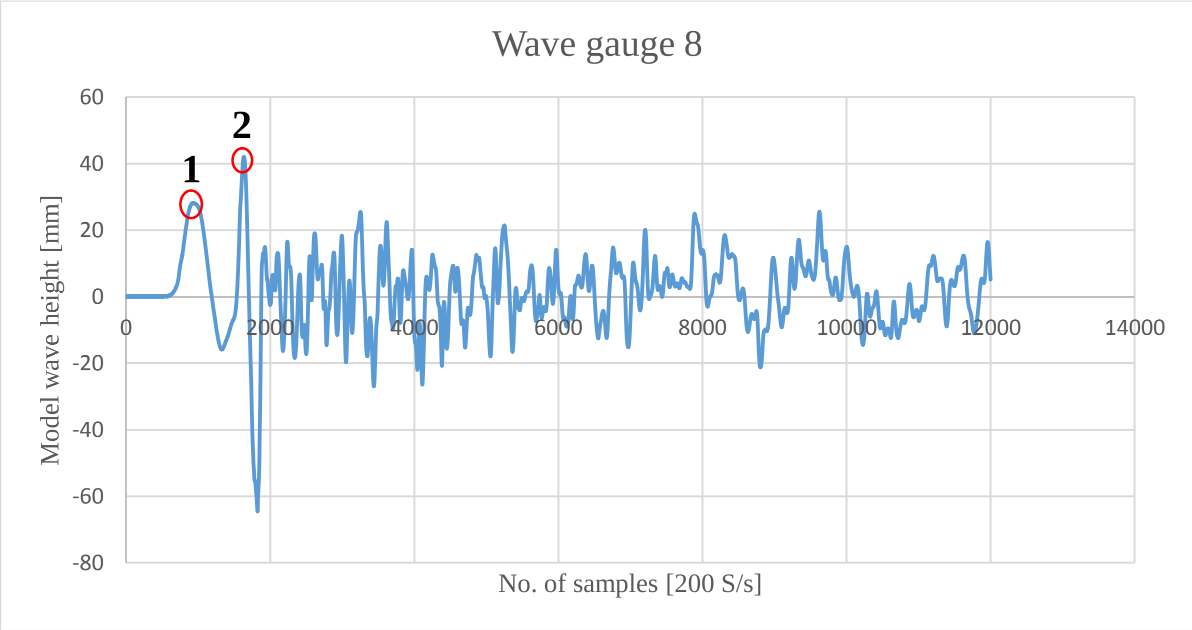

Figure 5-5 Wave gauge 8 measurements in HRWL case

On the contrary, in the HRWL case the traveling distance of the waves on the dam face is shorter and the highest registered overtopping wave is the second one.

5.2 Overtopping volume

Figure 5-6 shows the overtopping volume in prototype scale per meter of dam for each test.

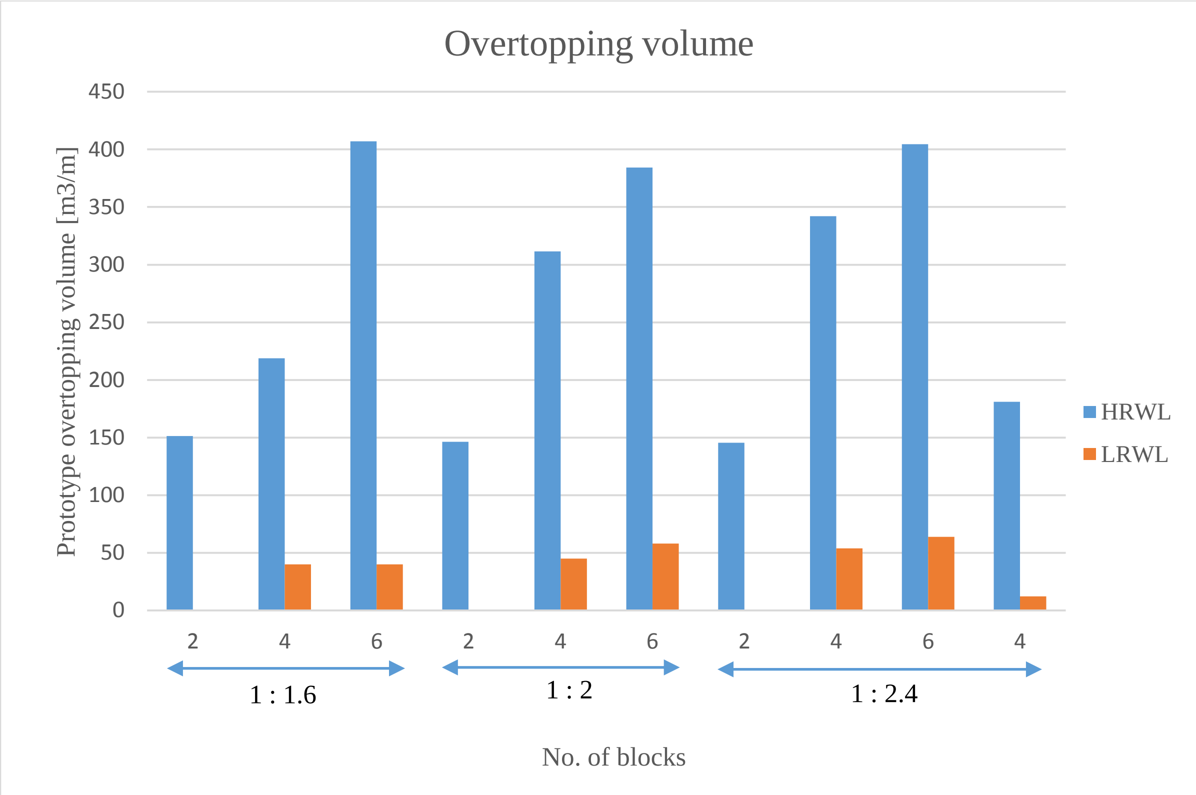

Figure 5-6 Measured overtopping volume in prototype scale

As expected, the results clearly show an increase of the overtopping when more blocks are added to the slide body; the six blocks slide generates an overtopping three times greater than the two blocks slide when the reservoir is at the highest regulated level.

On the other hand, the difference in overtopping in the lower reservoir level case is slight.

Analyzing Figure 5-6 is possible to see that the overtopping remains almost constant when decreasing the dam slope for the two and six blocks slide while it is increasing when the slide has four blocks. For the lower reservoir level case, the decrease of dam slope steepness causes a slight increase of the overtopping.

In order to fully understand these results, it is necessary to take into consideration the importance of freeboard and dam slope in the overtopping process. As clearly showed in the dam sketches, the traveling distance of the waves on the dam face increases when the dam slope becomes milder and it is even more affected when the freeboard is incremented, consequently limiting the overtopping volume.

5.3 Wave generation and propagation

Analyzing the video, it is possible to illustrate the process of wave generation.

In the instant of slide impact, the water spouts high and the water surface rises, creating the first wave. In the aftermath, as the slide is advancing into the bottom, a void is developed. The water spouts up again, flowing back and thus generating a lot of turbulence. The second wave is then originated. As the slide impact is very fast, a lot of spray is formed and some water even reaches the opposite bank.

The first wave has a smooth front, first impacting the opposite shore then proceeding towards the dam. On the other hand, the second wave has a broad and highly turbulent front. It is reflected many times by the model banks before reaching the dam. Afterwards, as the water surface becomes very turbulent, no other main wave fronts could be recognized.

Important information regarding the propagation process can also be obtained from the wave sensors.

Investigating the recorded data, it is possible to see that the second wave, which is the highest one, mainly propagates on the right side of the model (where gauge 3 and 6 are located) before being reflected by the banks and then hitting different sections of the dam.

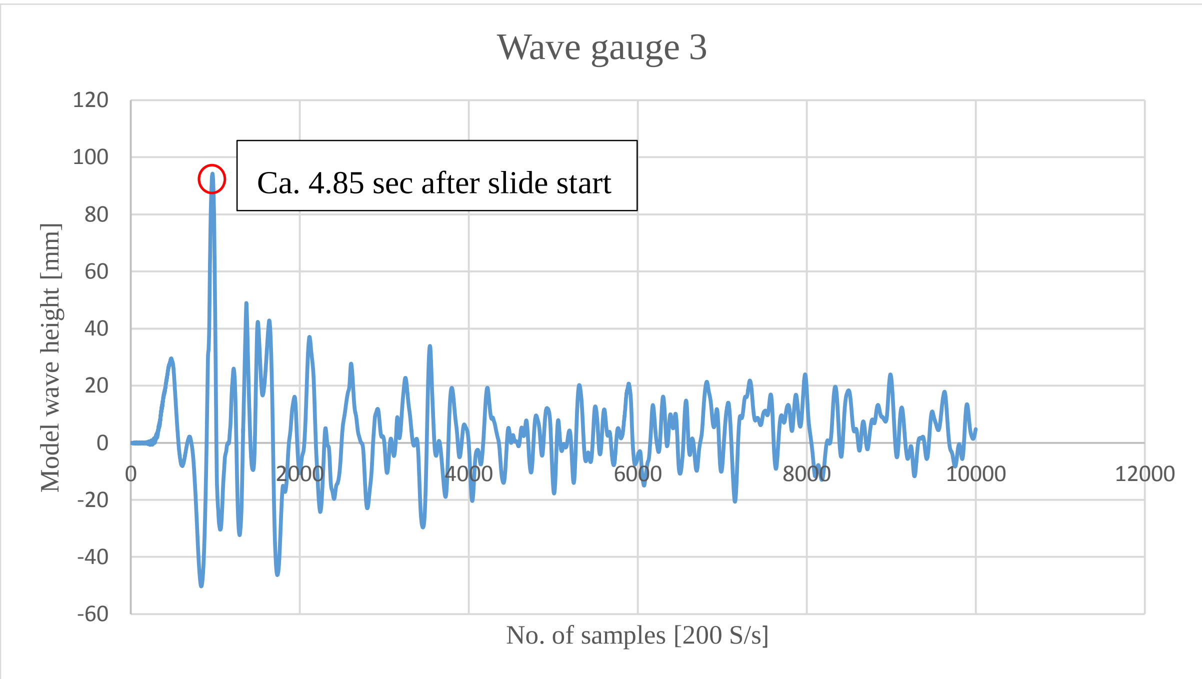

Figure 5-7 Wave gauge 3 measurements

After passing wave gauge 3, the wave continues to propagate on the right side of the model where the gauge 6 is located.

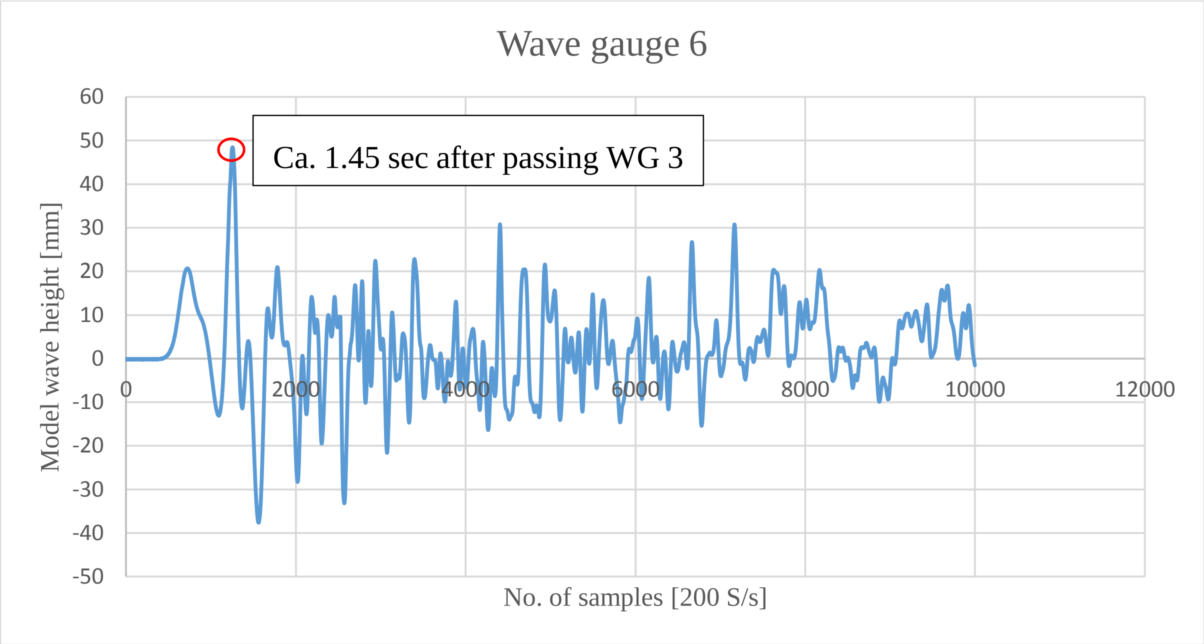

Figure 5-8 Wave gauge 6 measurements

5.4 Wave run-up and overtopping

The wave characteristics during the run-up process have been studied for both water levels cases.

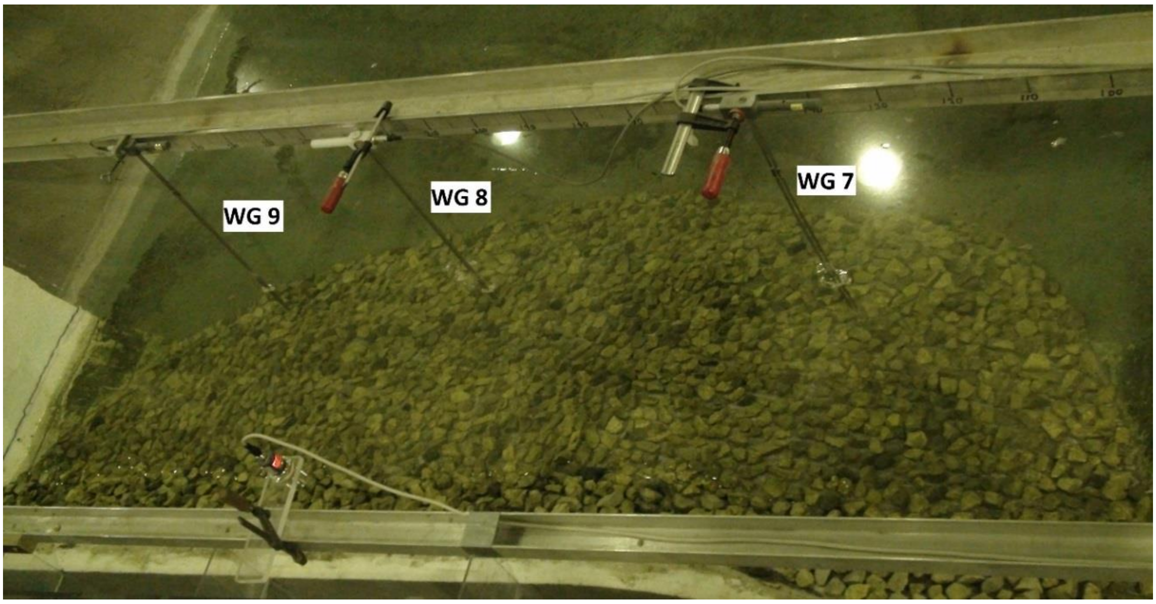

Figure 5-9 Location of WG 7, 8, 9

5.4.1 LRWL case

In order to study the run-up process, the data from the wave gauges 7, 8 and 9 have been analyzed.

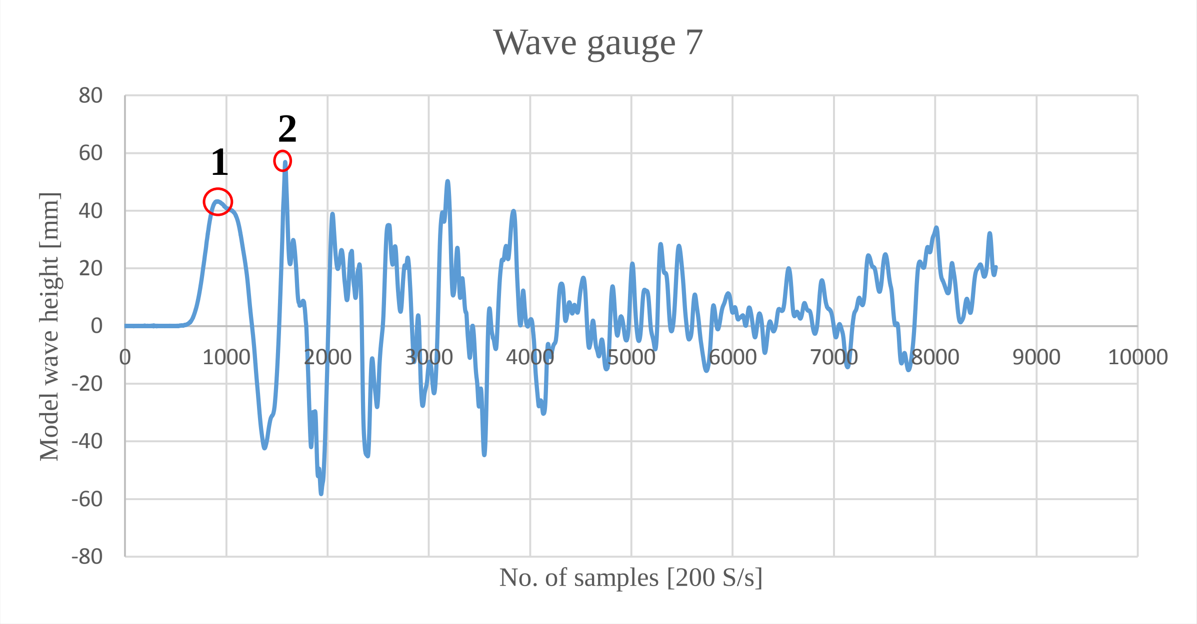

Figure 5-10 Wave gauge 7 measurements in the LRWL case

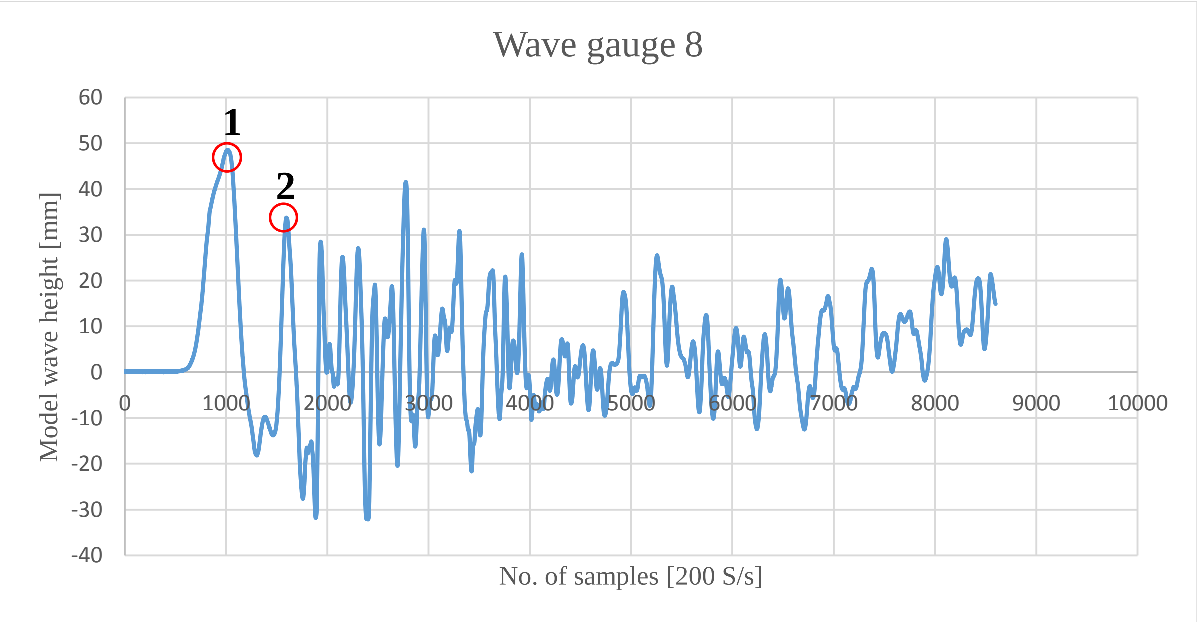

Figure 5-11 Wave gauge 8 measurements in the LRWL case

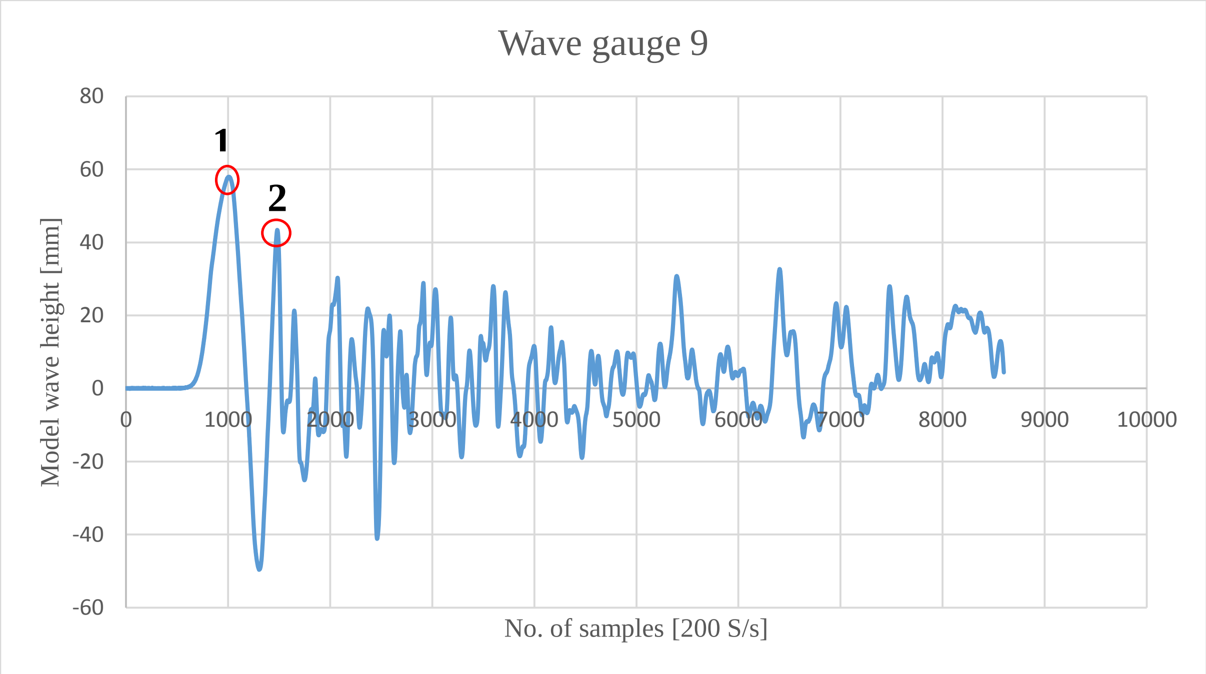

Figure 5-12 Wave gauge 9 measurements in the LRWL case

Analyzing the video and the data from the wave gauges located in front of the dam, only two main waves were identified in the LRWL case. The first one mainly impacts the middle and the right side of the dam while the second one hits the dam mostly on the left section.

5.4.2 HRWL case

In order to study the run-up process, the data from the wave gauges 7, 8 and 9 have been analyzed.

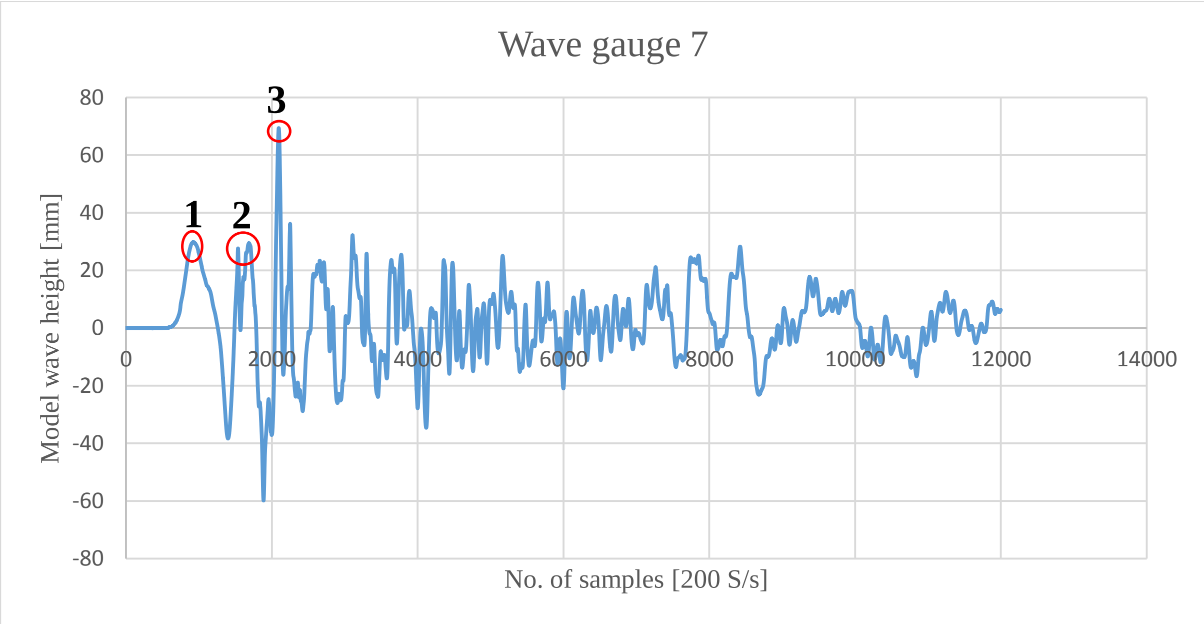

Figure 5-13 Wave gauge 7 measurements in the HRWL case

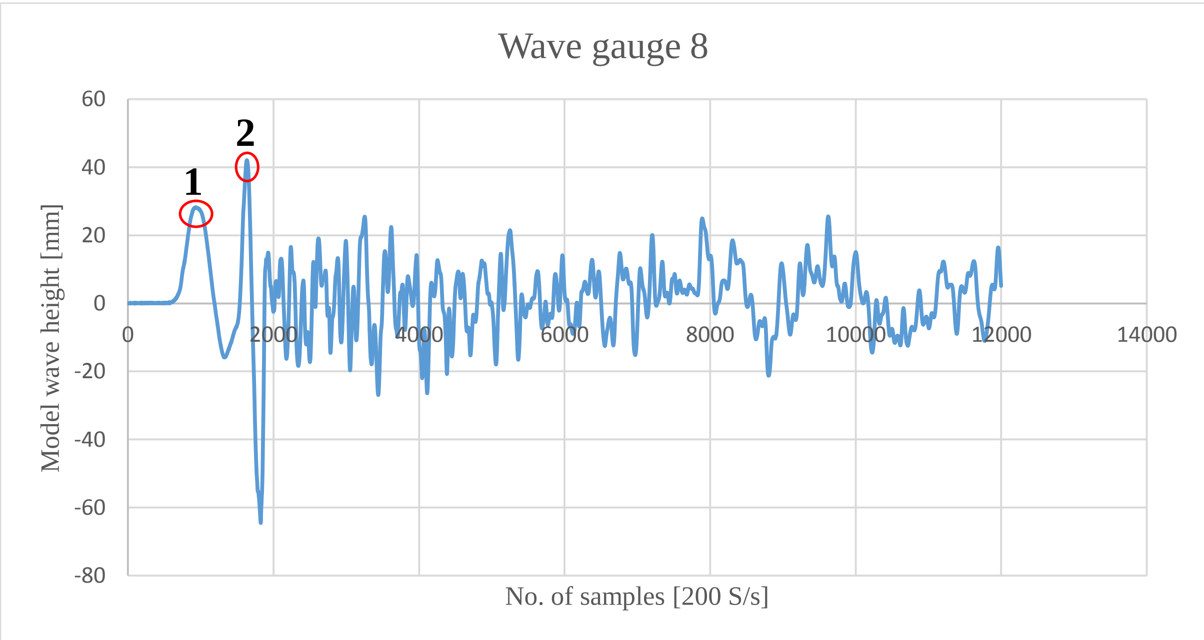

Figure 5-14 Wave gauge 8 measurements in the HRWL case

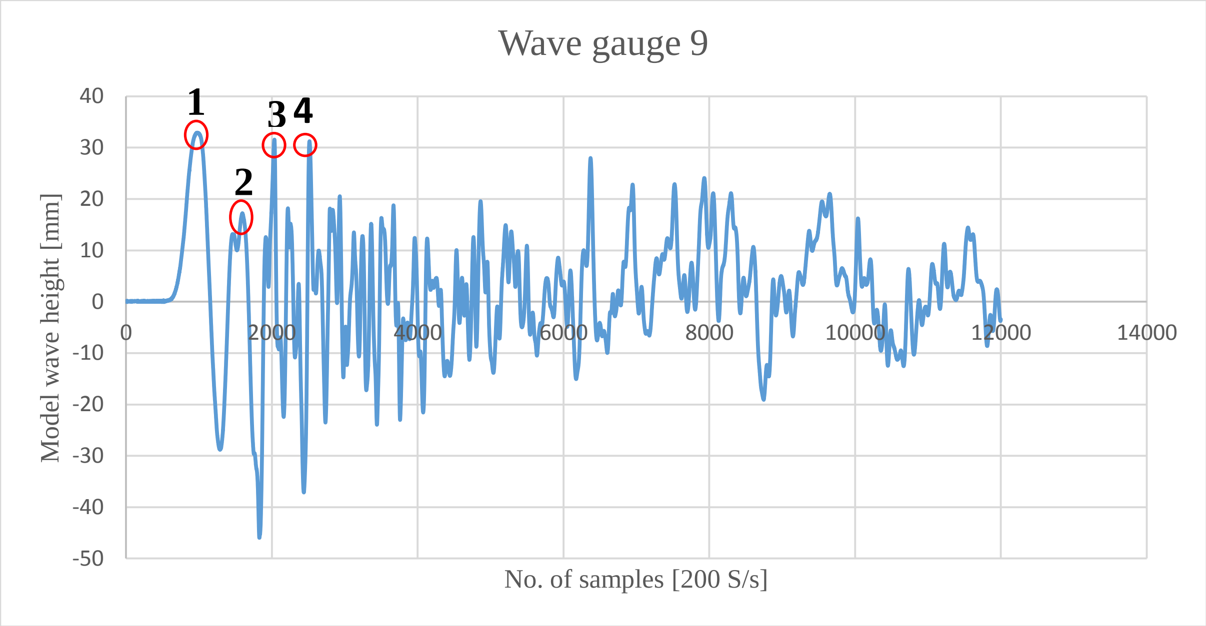

Figure 5-15 Wave gauge 9 measurements in the HRWL case

In the HRWL case three main waves were recognized. The first wave takes around 1 min (in prototype) after the slide to hit the dam, evenly overtopping throughout the dam width, while the second one mainly passes the dam in the middle. The third wave, identified as the highest one, impacts the dam 70 sec (in prototype) after the first wave and it is sectioned into a left and a right overtopping wave. In addition, a fourth wave overtops the dam on the right side. Afterwards no other main waves could be identified. It is then possible to conclude that the wave reflection at the shores has a strong influence on the wave propagation.

5.5 Estimation of overtopping height

As explained before, most of the overtopping takes place on the sides of the dam, therefore an estimation of the overtopping height on the external sections of the dam is performed for the HRWL case.

The overtopping volume from each sector of the dam is collected by the corresponding bucket, enabling the identification of the most loaded dam sections.

However, in order to obtain more precise results, it is recommended to place additional sensors.

The different dam sectors and the corresponding outlets are shown in Figure 5-16.

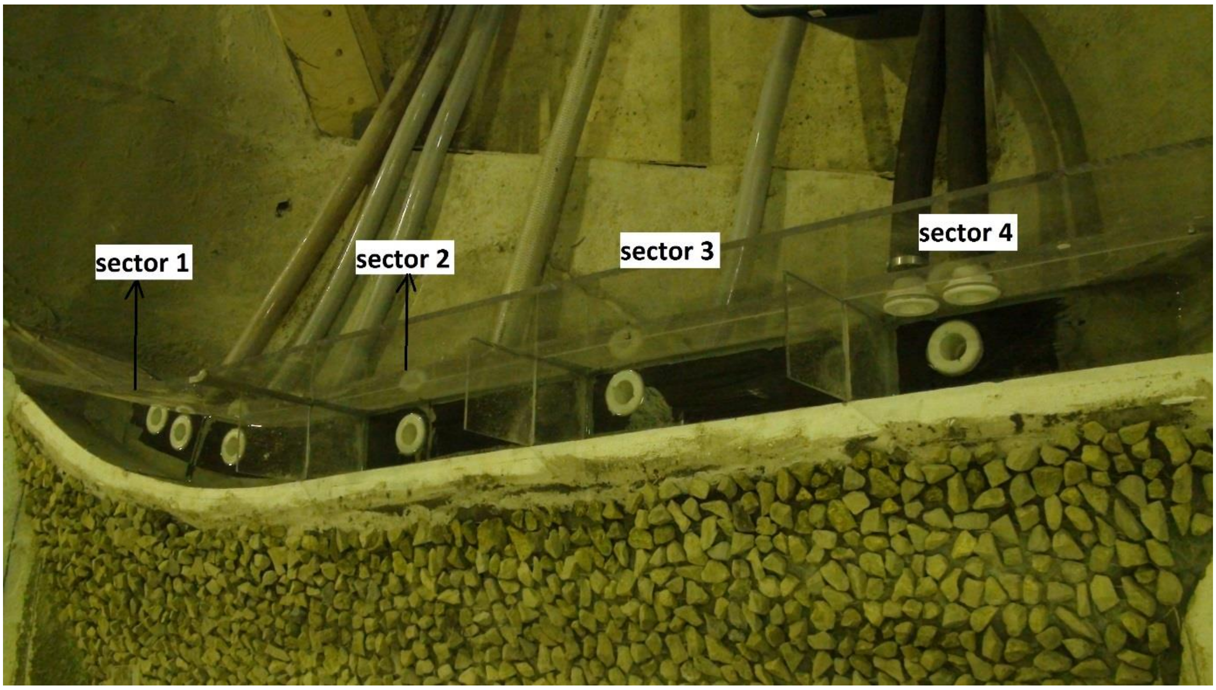

Figure 5-16 Dam sectors

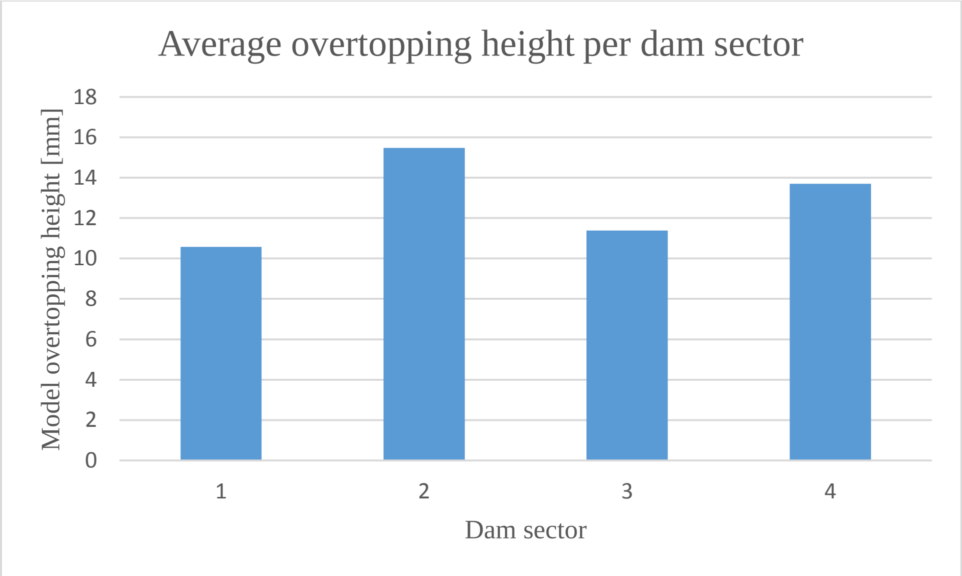

Figure 5-17 Average overtopping height per dam sector

As shown by Figure 5-17, the highest average overtopping height is located in the central sector. However, it has to be taken into consideration that sector 1, 3 and 4 are longer, therefore the local overtopping height will be considerably higher.

6 Comparison between observed and simulated data

The overtopping volume and the run-up height collected during the tests have also been compared with the results calculated with the Heller's numerical method.

6.1 Heller's numerical method

The Heller's method uses 15 easily measurable governing parameters to compute the overtopping volume and the run-up height caused by subaerial landslide generated waves. Furthermore, the main wave characteristics and the forces acting on the dam are also determined.

The method is divided in three phases: wave generation, wave propagation and wave run-up and overtopping. The calculations during the three phases are based on generally applicable equations; in addition, the method enables to compute the desired results for two different idealized reservoir geometry: channel (2D wave propagation) and basin (3D wave propagation).

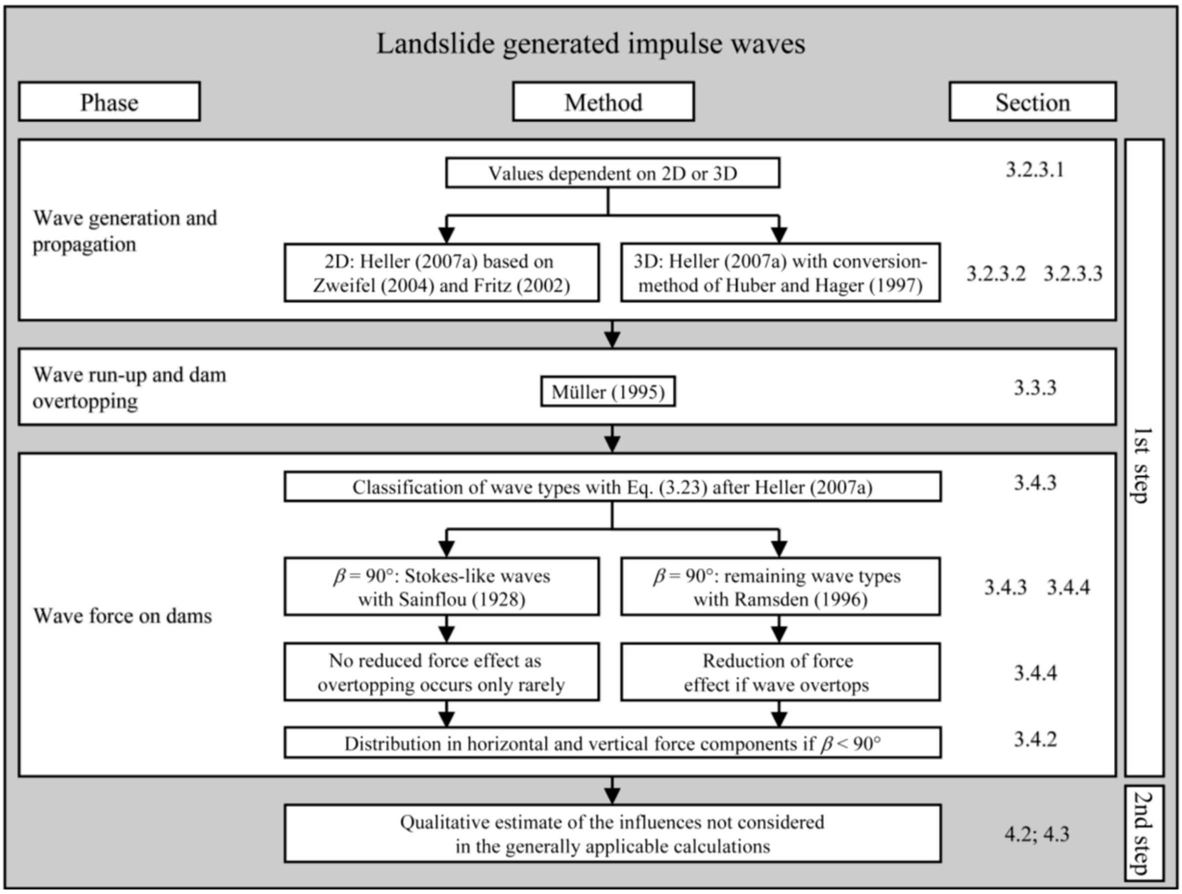

Figure 6-1 Phases of Heller's method (Heller et al., 2009)

An asset of the method is the introduction of the "impulse product parameter", a factor that contains all the governing parameters and therefore enables the prediction of most wave parameters.
However, the procedure requires that the parameters must be limited within certain ranges.

Term	Range	Meaning
Slide Froude number	$0.86 \leq \mathsf{F} \leq 6.83$	$\mathsf{F} = V_s/(gh)^{1/2}$
Relative slide thickness	$0.09 \leq S \leq 1.64$	$S = s/h$
Relative slide mass	$0.11 \leq M \leq 10.02$	$M = \rho_s \forall_s/(\rho_w bh^2)$
Relative slide density	$0.59 \leq D \leq 1.72$	$D = \rho_s/\rho_w$
Relative granulate density	$0.96 \leq \rho_g/\rho_w \leq 2.75$	ρ_g/ρ_w
Relative slide volume	$0.05 \leq V \leq 5.94$	$V = \forall_s/(bh^2)$
Bulk slide porosity	$30.7\% \leq n \leq 43.3\%$	n
Slide impact angle	$30° \leq \alpha \leq 90°$	α
Relative slide width	$0.74 \leq B \leq 3.33$	$B = b/h$
Relative radial distance	$5 \leq r/h \leq 30$	r/h
Wave propagation angle	$-90° \leq \gamma \leq +90°$	γ
Relative streamwise distance	$2.7 \leq X \leq 59.2$	$X = x/h$
Impulse product parameter	$0.17 \leq \mathsf{P} \leq 8.13$	$\mathsf{P} = \mathsf{F}S^{1/2}M^{1/4}\{\cos[(6/7)\alpha]\}^{1/2}$

Figure 6-2 Parameters limitations (Heller et al., 2009)

In order to obtain a more realistic approach, the 3D simulation has been chosen; however, it has to be taken into consideration that the ideal reservoir strongly differ from the natural one, where the bathymetry is very complex and effects such as shoaling, reflection and refraction are significant.

6.2 Run-up height

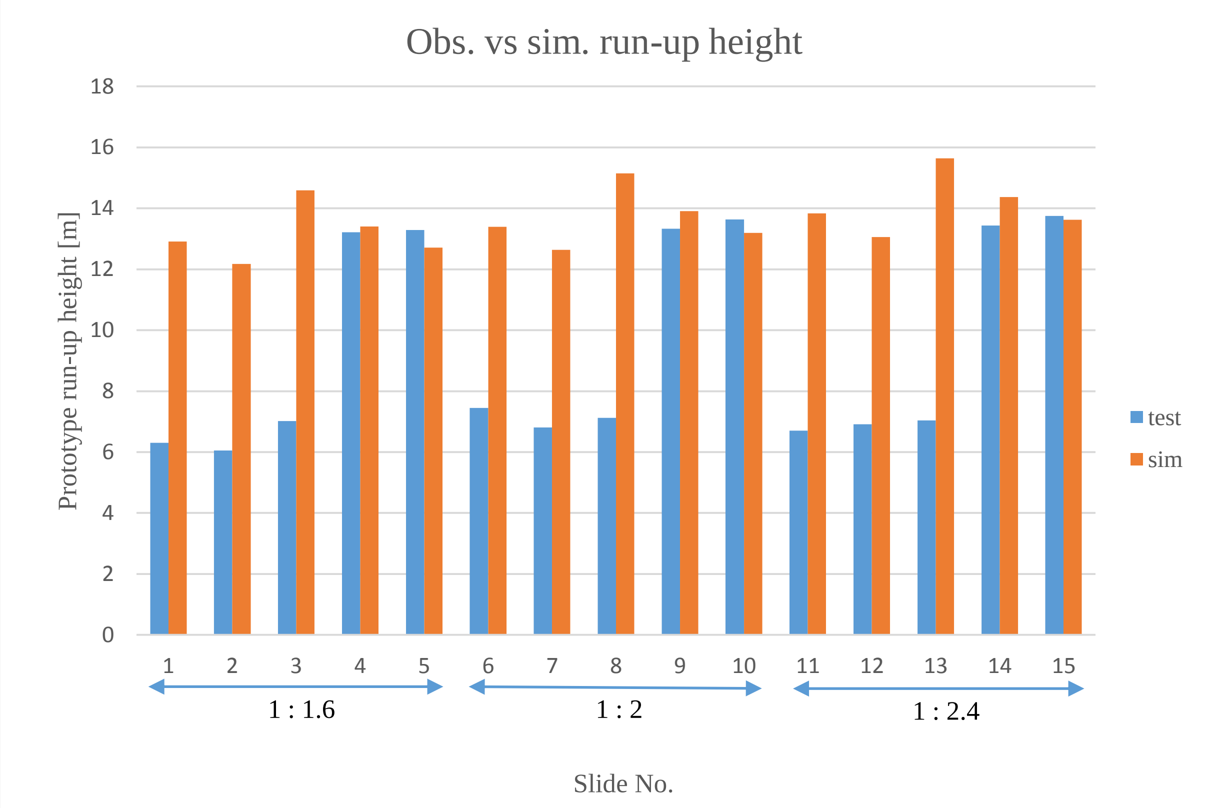

Figure 6-3 Comparison between observed and simulated run-up height

As shown in Figure 6-3, the Heller's method overestimates (ca. 45-50%) the run-up height in the HRWL case. While the numerical method calculates the maximum run-up height, the run-up height collected during the tests is not the maximum one because, as explained before, the highest run-up happens on the sides (in the HRWL case) while the sensor is placed in the middle of the dam. On the other hand, in the LRWL case a significant fraction of the wave run-up happens in the middle of the dam, therefore there is a better fit between observed and simulated data.

6.3 Overtopping volume

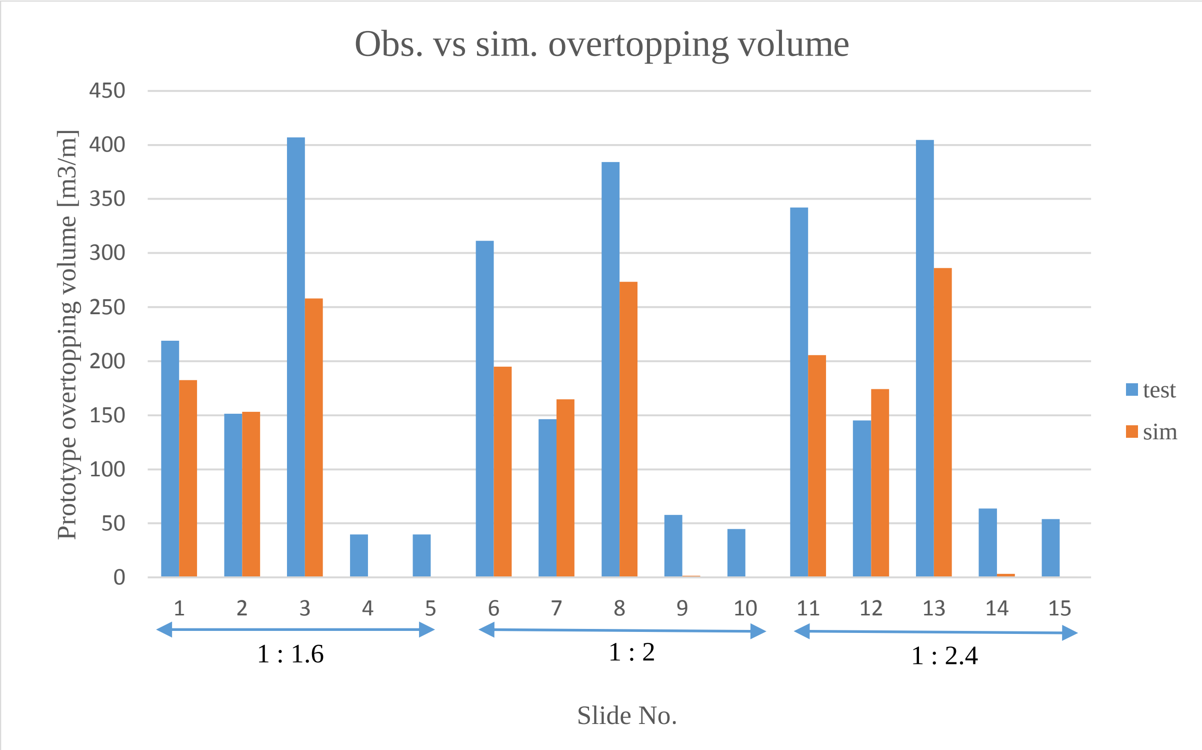

Figure 6-4 Comparison between observed and simulated overtopping volume

Analyzing Figure 6-4, it is possible to notice that the method underestimates the observed overtopping by approximately 30-35% in the 4 and 6 blocks cases, while for the 2 blocks slide there is a better fit between the observed and simulated overtopping values. In addition, in the LRWL case the method significantly underestimates the overtopping.

The poor fit of the simulated results is mainly due to the Heller's assumption of an idealized reservoir geometry. The method takes into consideration basin or channel with horizontal bed and straight banks. However, the Geiranger model has a complex bathymetry and constantly varying slopes which strongly affect the wave propagation and therefore the overtopping size. In addition, some of the parameter limitations were exceeded causing discrepancies between observed and simulated overtopping.

7 Conclusions and recommendations

7.1 Conclusions

The results of Chapter 5.2 show a strong correlation between the overtopping volume and the slide volume. In particular, the prototype overtopping varies in a range between 150 m^3/m, with a slide volume of 283991 m^3, and 400 m^3/m, with a slide volume of 851971 m^3.
It was also noticed the great influence of the freeboard on the overtopping size: when the freeboard height is increased by 7.9 m the measured overtopping decreases to 50 m^3/m.
Even though only two tests were performed, the impact of the upstream dam slope roughness is significant as it causes a 50 % reduction of the overtopping volume compared to the test with the same configuration.
On the other hand, the influence of the dam slope is minor, causing only slight changes in the overtopping volume.
The prototype run-up height presented in Chapter 5.1 varies between 6 m (HRWL case) and 13.8 m (LRWL case). No strong correlations between the parameters have been found.

The results of Chapter 6 show large discrepancies between observed and simulated data. The main reason is the method assumption of an idealized reservoir geometry which strongly differ from the Geiranger model geometry, where the bottom and the banks constantly vary, affecting the wave propagation and the overtopping. The video analysis and the wave gauges inspection show that the run-up process is highly influenced by the reservoir shape: after the slide impact the waves propagate in the reservoir being reflected several times by the model banks and then unevenly impacting the different sections of the dam. In particular it was noticed the different behavior of the run-up waves in the two water levels cases.

7.2 Recommendations

In order to improve the accuracy of the estimate of the overtopping, two possible alternatives are presented.
The first one is to test the applicability of the Heller's method by using a model with an idealized reservoir geometry; the advantage of this option is that the processes of wave propagation and run-up would be considerably simplified and easier to study as the influence of the reservoir geometry would be extremely lower. However, the drawback of this alternative is that the collected data cannot be used to estimate the overtopping in natural reservoir conditions.

The second option, although it is time consuming, is to develop a new method that takes into consideration the characteristics of Viddal reservoir, enabling to obtain a more accurate estimate of the size of the overtopping.

Three recommendations are given for the model test:

- As the wave run-up on the sides of the dam is significant, it is recommended to place additional sensors on the external sections of the dam in order to have a better understanding of the run-up process.
- Since the freeboard is one of the most sensible parameter regarding the size of the overtopping, it is then advised to increase it in respect of dam safety.
- As a last recommendation, it is strongly suggested to conduct more tests with upstream dam slope roughness in order to have a better understanding of its impact on the overtopping process.

8 References

Heller, V., Hager, W. H., & Minor, H.-E. (2009). Landslide generated impulse waves in reservoirs: Basics and computation.

Kamphuis, J., & Bowering, R. (1970). Impulse waves generated by landslides. *Coastal Engineering Proceedings, 1*(12).

Müller, D. (1995). Auflaufen und Überschwappen von Impulswellen an Talsperren. VAW-Mitteilung 137, Ed. Vischer D, Versuchsanstalt für Wasserbau, Hydrologie und Glaziologie, ETH Zürich.

Panizzo, A., De Girolamo, P., & Petaccia, A. (2005). Forecasting impulse waves generated by subaerial landslides. *Journal of Geophysical Research: Oceans (1978–2012), 110*(C12).

Schuster, R. L., & Wieczorek, G. F. (2002). *Landslide triggers and types.* Paper presented at the Landslides: proceedings of the first European conference on landslides, Taylor & Francis, Prague.

Teng, M. H., Feng, K., & Liao, T. I. (2000). *Experimental study on long wave run-up on plane beaches.* Paper presented at the The Tenth International Offshore and Polar Engineering Conference.

Varnes, D. J. (1958). Landslide types and processes. *Highway Research Board Special Report*(29).

Appendix A

The slide characteristics for each test are presented.

TEST 1			
Properties	**Unit**	**Model**	**Prototype**
Volume	m3	0.1485	567981
Width	m	0.9	142.2
Thickness	m	0.16	25.28
Porosity	%	0	0
Density	g/cm3	1.077	1.077
Impact velocity	m/s	2.387	30.071
No. of blocks	-	4	
Freeboard	m	0.03	5
Dam slope	°	32	

TEST 2			
Properties	**Unit**	**Model**	**Prototype**
Volume	m3	0.072	283991
Width	m	0.9	142.2
Thickness	m	0.16	25.28
Porosity	%	0	0
Density	g/cm3	1.046	1.046
Impact velocity	m/s	2.546	32.076
No. of blocks	-	2	
Freeboard	m	0.03	5
Dam slope	°	32	

TEST 3			
Properties	**Unit**	**Model**	**Prototype**
Volume	m3	0.225	851971
Width	m	0.9	142.2
Thickness	m	0.16	25.28
Porosity	%	0	0
Density	g/cm3	1.088	1.088
Impact velocity	m/s	2.323	29.276
No. of blocks	-	6	
Freeboard	m	0.03	5
Dam slope	°	32	

TEST 4			
Properties	**Unit**	**Model**	**Prototype**
Volume	m3	0.225	851971
Width	m	0.9	142.2
Thickness	m	0.16	25.28
Porosity	%	0	0
Density	g/cm3	1.088	1.088
Impact velocity	m/s	2.367	29.825
No. of blocks	-	6	
Freeboard	m	0.08	12.9
Dam slope	°	32	

TEST 5			
Properties	**Unit**	**Model**	**Prototype**
Volume	m3	0.149	567981
Width	m	0.9	142.2
Thickness	m	0.16	25.28
Porosity	%	0	0
Density	g/cm3	1.077	1.077
Impact velocity	m/s	2.415	30.435
No. of blocks	-	4	
Freeboard	m	0.08	12.9
Dam slope	°	32	

TEST 6			
Properties	**Unit**	**Model**	**Prototype**
Volume	m3	0.1485	567981
Width	m	0.9	142.2
Thickness	m	0.16	25.28
Porosity	%	0	0
Density	g/cm3	1.077	1.077
Impact velocity	m/s	2.458	30.965
No. of blocks	-	4	
Freeboard	m	0.03	5
Dam slope	°	26.57	

TEST 7			
Properties	**Unit**	**Model**	**Prototype**
Volume	m3	0.072	283991
Width	m	0.9	142.2
Thickness	m	0.16	25.28
Porosity	%	0	0
Density	g/cm3	1.046	1.046
Impact velocity	m/s	2.626	33.083
No. of blocks	-	2	
Freeboard	m	0.03	5
Dam slope	°	26.57	

TEST 8			
Properties	**Unit**	**Model**	**Prototype**
Volume	m3	0.225	851971
Width	m	0.9	142.2
Thickness	m	0.16	25.28
Porosity	%	0	0
Density	g/cm3	1.088	1.088
Impact velocity	m/s	2.237	28.19
No. of blocks	-	6	
Freeboard	m	0.03	5
Dam slope	°	26.57	

TEST 9			
Properties	**Unit**	**Model**	**Prototype**
Volume	m3	0.225	851971
Width	m	0.9	142.2
Thickness	m	0.16	25.28
Porosity	%	0	0
Density	g/cm3	1.088	1.088
Impact velocity	m/s	2.26	28.479
No. of blocks	-	6	
Freeboard	m	0.08	12.9
Dam slope	°	26.57	

TEST 10			
Properties	**Unit**	**Model**	**Prototype**
Volume	m3	0.149	567981
Width	m	0.9	142.2
Thickness	m	0.16	25.28
Porosity	%	0	0
Density	g/cm3	1.077	1.077
Impact velocity	m/s	2.364	29.782
No. of blocks	-	4	
Freeboard	m	0.08	12.9
Dam slope	°	26.57	

TEST 11			
Properties	**Unit**	**Model**	**Prototype**
Volume	m3	0.1485	567981
Width	m	0.9	142.2
Thickness	m	0.16	25.28
Porosity	%	0	0
Density	g/cm3	1.077	1.077
Impact velocity	m/s	2.298	28.95
No. of blocks	-	4	
Freeboard	m	0.03	5
Dam slope	°	22.62	

TEST 12			
Properties	**Unit**	**Model**	**Prototype**
Volume	m3	0.072	283991
Width	m	0.9	142.2
Thickness	m	0.16	25.28
Porosity	%	0	0
Density	g/cm3	1.046	1.046
Impact velocity	m/s	2.497	31.464
No. of blocks	-	2	
Freeboard	m	0.03	5
Dam slope	°	22.62	

TEST 13			
Properties	**Unit**	**Model**	**Prototype**
Volume	m3	0.225	851971
Width	m	0.9	142.2
Thickness	m	0.16	25.28
Porosity	%	0	0
Density	g/cm3	1.088	1.088
Impact velocity	m/s	2.292	28.881
No. of blocks	-	6	
Freeboard	m	0.03	5
Dam slope	°	22.62	

TEST 14			
Properties	**Unit**	**Model**	**Prototype**
Volume	m3	0.225	851971
Width	m	0.9	142.2
Thickness	m	0.16	25.28
Porosity	%	0	0
Density	g/cm3	1.088	1.088
Impact velocity	m/s	2.294	28.907
No. of blocks	-	6	
Freeboard	m	0.08	12.9
Dam slope	°	22.62	

TEST 15			
Properties	**Unit**	**Model**	**Prototype**
Volume	m3	0.149	567981
Width	m	0.9	142.2
Thickness	m	0.16	25.28
Porosity	%	0	0
Density	g/cm3	1.077	1.077
Impact velocity	m/s	2.393	30.154
No. of blocks	-	4	
Freeboard	m	0.08	12.9
Dam slope	°	22.62	

TEST 16			
Properties	**Unit**	**Model**	**Prototype**
Volume	m3	0.1485	567981
Width	m	0.9	142.2
Thickness	m	0.16	25.28
Porosity	%	0	0
Density	g/cm3	1.077	1.077
Impact velocity	m/s	2.393	30.154
No. of blocks	-	4	
Freeboard	m	0.08	12.9
Dam slope	°	22.62	
Upstream dam slope roughness			

TEST 17			
Properties	**Unit**	**Model**	**Prototype**
Volume	m3	0.149	567981
Width	m	0.9	142.2
Thickness	m	0.16	25.28
Porosity	%	0	0
Density	g/cm3	1.077	1.077
Impact velocity	m/s	2.298	28.95
No. of blocks	-	4	
Freeboard	m	0.03	5
Dam slope	°	22.62	
Upstream dam slope roughness			

Appendix B

Data collected from the measurements devices (test 6).

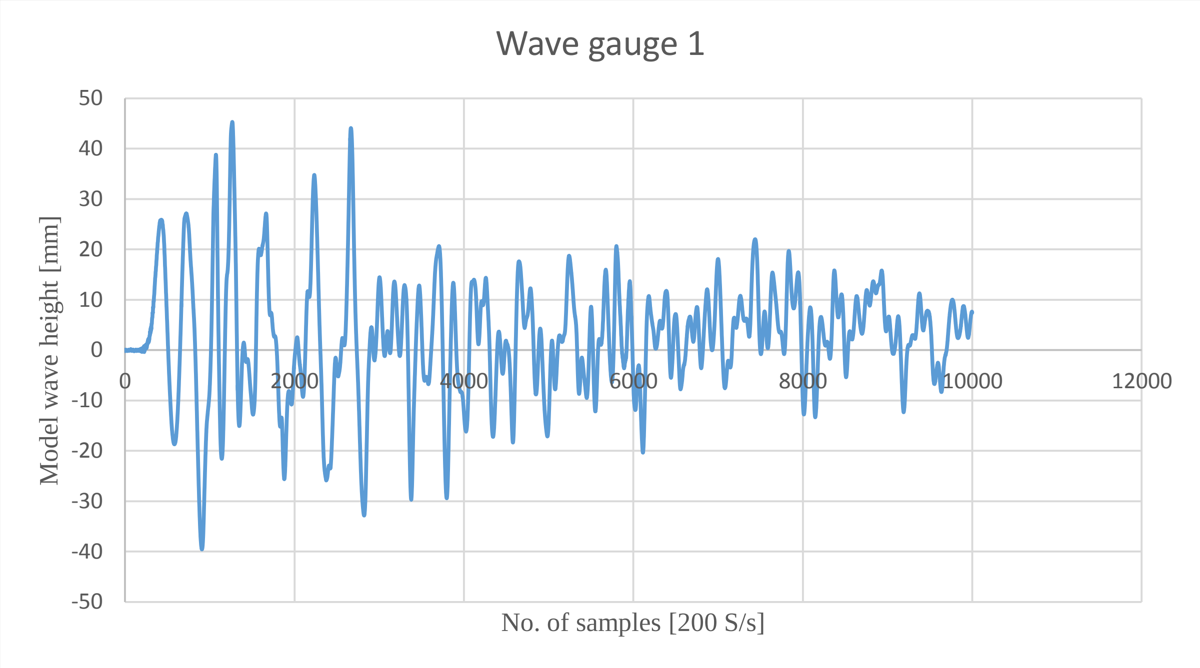

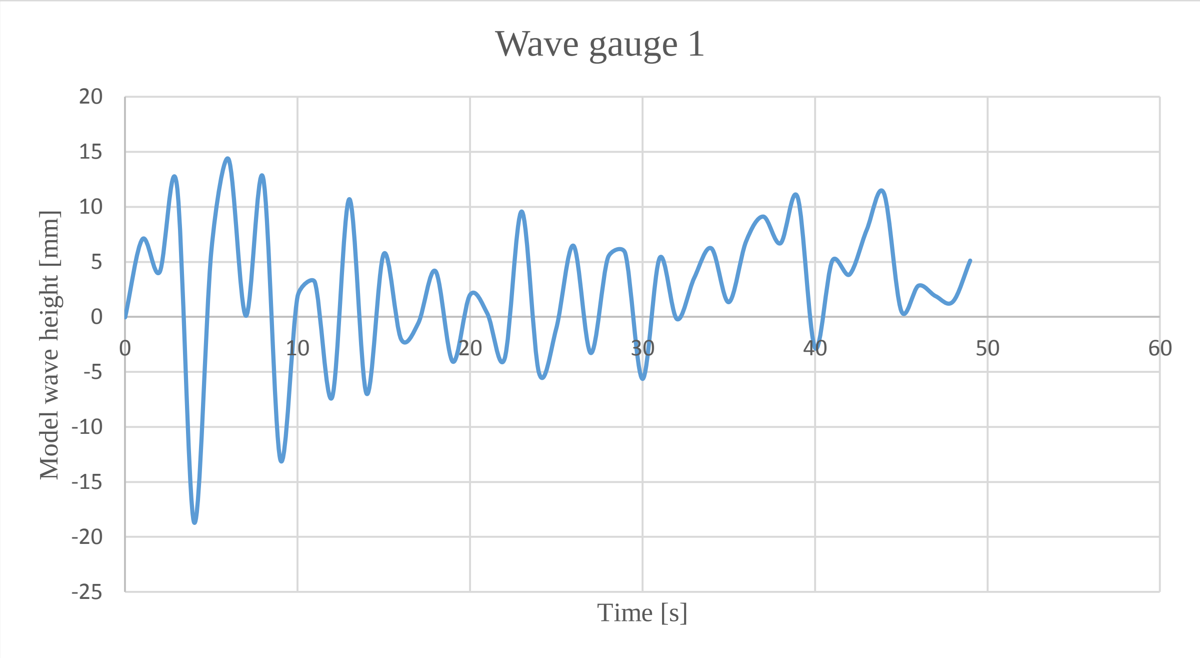

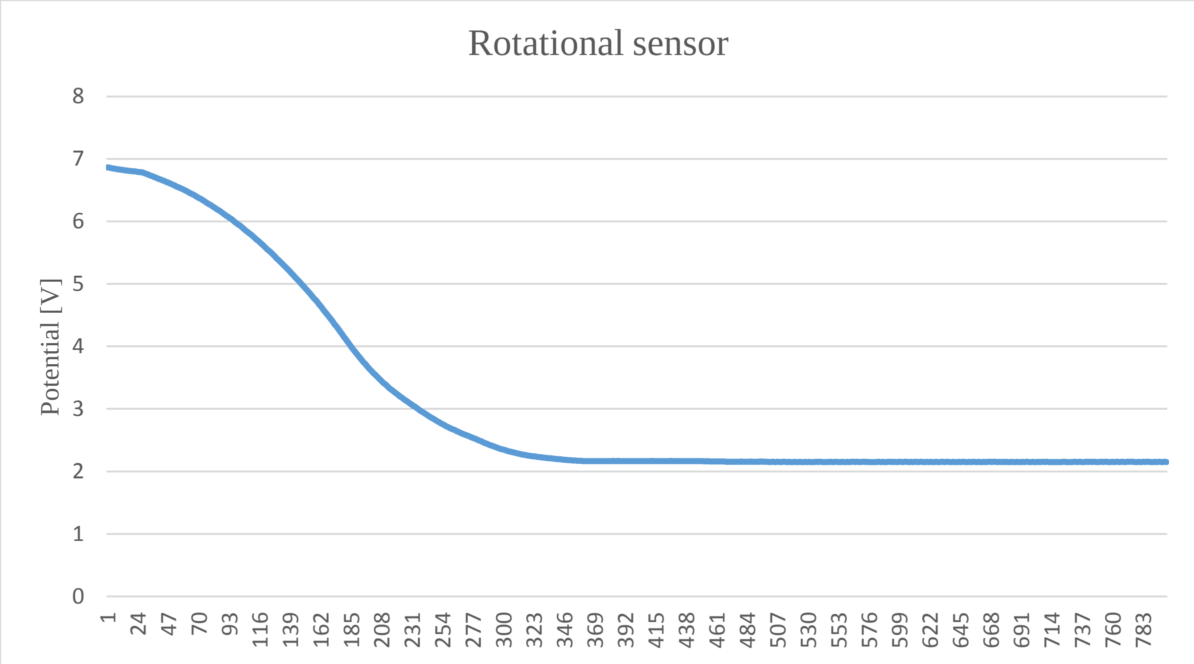
Rotational sensor
Potential [V]
8
7
6
5
4
3
2
1
0
1
24
47
70
93
116
139
162
185
208
231
254
277
300
323
346
369
392
415
438
461
484
507
530
553
576
599
622
645
668
691
714
737
760
783

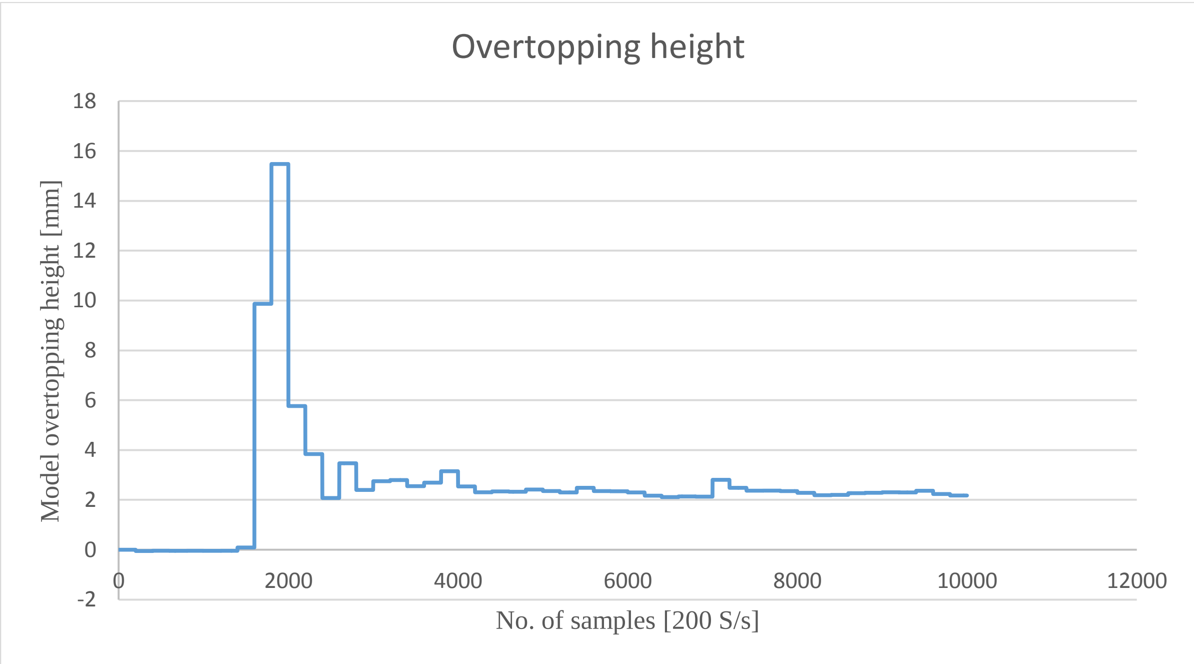
Overtopping height
Model overtopping height [mm]
18
16
14
12
10
8
6
4
2
0
-2
0
2000
4000
6000
8000
10000
12000
No. of samples [200 S/s]

Appendix C

Excel sheet from Heller's numerical method (test 6).

Landslide generated impulse waves in reservoirs - Basics and computation Spread sheets			
Project name	Landslide	Operator	Matteo Bolzoni
Computational point	Test 6	Date	03.05.2015
Governing parameters			
Wave generation (Subsection 3.2.2)			
Slide impact velocity V_s [m/s]	56	Bulk slide density ρ_s [kg/m^3]	1 077
Bulk slide volume Ɐ_s [m^3]	567 981	Bulk slide porosity n [%]	0
Slide thickness s [m]	25	Slide impact angle α [°]	42
Slide or reservoir width b [m]	142	Still water depth h [m]	88
Wave propagation (3D or 2D) (Subsection 3.2.2)			
Wave basin (3D)		Wave channel (2D)	
Radial distance r [m]	1 011	Streamwise distance x [m]	-
Wave propagation angle γ [°]	-81		
Wave run-up and overtopping (Subsection 3.3.2)			
Still water depth h [m]	57	Freeboard f [m]	5
Run-up angle β [°]	27	Crest width b_K [m]	5
Main results			
Wave heigth H (H_M) [m]			7.4
Wave amplitude a (a_M) [m]			5.9
Wave period T (T_M) [s]			21.7
Wave length L (L_M) [m]			538.3
Run-up height R [m]			13.4
Overtopping volume Ɐ_0 per unit length dam crest for f = 0 [m^3/m]			545.1
Duration of overtopping t_0 for f = 0 [s]			25.6
Average discharge q_{0m} per unit length dam crest for f = 0 [m^2/s]			21.3
Maximum discharge q_{0M} per unit length dam crest for f = 0 [m^2/s]			42.6
Overtopping volume per unit length dam crest Ɐ [m^3/m]			195.1
Hor. force comp. p.u.l. dam crest resulting only from hydrostatic pressure $K_{RW,h}$ [N/m]			15 936 345
Ver. force comp. p.u.l. dam crest resulting only from hydrostatic pressure $K_{RW,v}$ [N/m]			31 865 809
Wave type (Stokes-like wave 3.4.3 or remaining wave types 3.4.4)			Stokes
Remaining: total horizontal force component per unit length dam crest resulting from an impulse wave and hydrostatic pressure $K_{tot,h}$ [N/m]			No value
Remaining: reduced total horizontal force component per unit length dam crest resulting from an impulse wave and hydrostatic pressure $K_{tot,h,abg}$ [N/m]			No value
Remaining: elevation $z_{K,tot,h,abg}$ of the resultant of $K_{tot,h,abg}$ [m]			No value
S/r: additional hor. force comp. p.u.l. dam crest resulting from impulse wave ΔK_h [N/m]			4 113 975
Stokes: elevation $z_{\Delta K,h}$ of the resultant of ΔK_h [m]			31.8
S/r: ad. vertical force component p.u.l. dam crest resulting from impulse wave ΔK_v [N/m]			8 226 173
Limitations			
Number of not satisfied limitations out of 23 (2D) or 24 (3D), respectively			4

Appendix D

The content of the attached CD is presented below.

- photo
- video
- data collection
- freeboard
- model sketch
- model-prototype
- obs-sim
- overtopped volume
- simulated data
- test1
- test2
- test3
- test4
- test5
- test6
- test7
- test8
- test9
- test10
- test11
- test12
- test13
- test14
- test15
- test16
- test17